Title: Light-responsive nanomaterials with pro-oxidant and anti-oxidant activity.

Authors: Soumik Podder[1,2,*], Chandan Kumar Ghosh[2], Avijit Das[1], John George Hardy[3,4,*]

Affiliations:

1. Department of Electronics and Communication Engineering, Guru Nanak Institute of Technology, Kolkata-700114, India
2. School of Materials Science and Nanotechnology, Jadavpur University, India
3. Department of Chemistry, Lancaster University, Lancaster, Lancashire LA1 4YB, U.K
4. Materials Science Institute, Lancaster University, Lancaster, Lancashire LA1 4YB, U.K

*Corresponding authors: nanotechsoumik@gmail.com (S.P.); j.g.hardy@lancaster.ac.uk (J.G.H.)

Abstract

Nanomaterials are capable of generating reactive oxygen species (ROS) due to defect induced electronic interactions with oxygen and water stimulated by environmental and structural factors (e.g., photonic energy, band edge energy and morphology) resulting in excellent pro-oxidant activity of nanomaterials. The pro-oxidant activities are demonstrated by the antibacterial activity of nanomaterials under different environmental conditions (e.g., varying light levels). This review examines research related to the pro-oxidant activity of metallic, non-metallic, metal oxide nanoparticles (NPs) and their composites. Moreover, there is a scavenging phenomenon for nanomaterials that manifests itself as inhibition of ROS (i.e., anti-oxidant activity) which is also dependent on the electronic property of the nanomaterials, which is examined. These nanomaterials experience a crossover between pro-oxidant and anti-oxidant activities depending on concentration, morphology etc., which offers the nanomaterials potential for application in cancer therapy and inflammatory disease treatment.

Keywords: Prooxidant activity, Antioxidant activity, Metal Oxide, ROS, Antibacterial activity

Introduction

Nanomaterials tend to have high surface/volume ratios and opportunities for enrichment with various defect related properties,[**1**] potentially enabling the generation of reactive oxygen species (ROS).[**2**] ROS are primarily generated from nanomaterials after light excitement whose energy level is higher than the band gap of the nanomaterial,[**3**] and can be generated in dark too due to presence of defect states [**4,5**] The photometric excitement generates electron-hole pairs that eventually recombine with each other resulting in the emission of photons[**2**] but defect states of nanomaterial can trap these charge carriers where their lifetimes are many times longer than triplet states of dyes[**6**] and thus lower the chance of recombination of photogenerated electron-hole pairs, thereby offering opportunities to react with adsorbed species (molecular oxygen, water molecules, etc.) on the surface of the nanomaterials producing ROS.[**2**] The ROS generation occurs either when electrons are donated to molecular oxygen or other acceptors(a reductive process) and when holes are

transferred to an electron donor (an oxidative process).[**2**] Various types of primary ROS are produced by nanomaterials notably superoxide anions ($O_2^{\cdot-}$), hydroxyl radicals ($^{\cdot}OH$) and singlet oxygen ($^1O_2$).[**7**] Various types of secondary ROS are produced by nanomaterials, particularly hydroperoxyl radicals ($^{\cdot}HO_2$) generated from $O_2^{\cdot-}$ by a reductive process.[**8**] The overall processes are summarized below in equations .[**9,10**]

$$O_2 + e^- \rightarrow O_2^{\cdot-} \quad (1)$$

$$O_2^{\cdot-} + H_2O \rightarrow \cdot HO_2 + OH^- \quad (2)$$

$$\cdot HO_2 + \cdot HO_2 \rightarrow H_2O_2 \quad (3)$$

$$H_2O_2 + O_2^{\cdot-} \rightarrow O_2 + \cdot OH + OH^- \quad (4)$$

$$h^+ + (H_2O)_{ads} \rightarrow h^+ + (H^+ + OH^-)_{ads} \rightarrow \cdot OH + H^+ \quad (5)$$

$$h^+ + O_2^{\cdot-} \rightarrow 1O_2 \quad (6)$$

$$h^+ \rightarrow hole \qquad e^- \rightarrow electron$$

The generation of ROS in nanomaterials produces oxidative stress which is the primary cause of nanotoxicity. [**2,7,10**]

The pro-oxidant activity of nanomaterials is an interesting field of studies where the primary aim is to elucidate the interaction of nanomaterials with biological entities (e.g., molecules, cells, tissues, organs, etc.). This physiological interaction involves a variety of physiological processes such as absorption, distribution, metabolism, excretion, cellular uptake and trafficking, toxicity, etc.[**11**] The pro-oxidant potential of nanomaterials are dependent on various physicochemical properties including chemical composition, size, shape, surface chemistry, zeta potential, crystallinity, solubility, redox potential, etc [**12**] and a thorough understanding of these properties helps to analyze plausible nano-bio interactions and inform the design of biocompatible products. The toxicity of materials can be due to the interactions of nanoscale entities with biological entities, potentially resulting in effects including, but not limited to, antibacterial activity and ROS mediated cancer therapy that have captured the attention of researchers and practitioners worldwide, due to the potential applications of such nanomaterials in advanced technologies.[**13**] One biomedically relevant example is endodontic applications, where nanomaterials with antibacterial properties are particularly interesting, as indeed are multifunctional materials [**14**] Another biomedically relevant example is anticancer applications, where the pro-oxidant activity of nanomaterials is cytotoxic and genotoxic towards cancer cells, and particularly potent when coupled with targeted drug delivery. [**15, 16, 17, 18**]

The pro-oxidant activity of nanomaterials results in $^1O_2$ injection which can kill cancer cells. [**19, 20, 21**]

The antioxidant activity of a material is defined by its ability to inhibit the autoxidation of entities including: lipids (triglycerides, cholesterol), proteins, carbohydrates, etc.[**22**]. In live cells the ROS level is maintained by different intracellular enzymes, including: superoxide dismutase (SOD), peroxidase (POD), catalase and extracellular enzymes such as vitamin C, E and coenzymes [**23**] but these natural antioxidants/enzymes are characterized by poor chemical stability and bioavailability on demand (due to low production, poor solubility and

low cellular uptake) [**24**] Nanomaterials have the potential to overcome these challenges; indeed, defect-induced electronic structures enable nanomaterials to slow down the autoxidation process by trapping chain carrying radicals at defect states and thus behave as nanoantioxidants [**22**]

The antioxidant properties of nanomaterials challenges the limitations of traditional chemotherapies for cancer where the ROS scavenging mechanism can protect normal cell[**25**] ROS scavenging can also be helpful in reducing inflammation that potentially finds application in wound healing[**26**] regenerative medicine[**27**],tissue engineering[**28**] etc. It is noteworthy that the pro-oxidant and anti-oxidant activities of nanomaterials depend on several parameters such as particle size, morphology, concentration, illumination etc. [**29**] which will play a role in the context in which they can be applied.

This review highlights the ROS generation ability of different nanomaterials such as metallic, non-metallic and metal oxide with their composites. ROS production and electronic structure of nanomaterials are correlated, as are implications for the antibacterial and anticancer activities, and antioxidant behavior and the crossover approach which may be helpful for researchers to design and develop new kinds of advanced nanomedicines.

Metallic NPs

Conventionally metallic NPs are differed from semiconducting materials in regards of band gap energy that may make inquiries of ROS generation ability. These NPs are extensively employed in various biological applications including antimicrobial, cancer therapy etc due to their toxicity.[**30-33**] Fortunately there is abundant literature detailing ROS generation and related oxidative stress induced cytotoxicity of metallic NPs.[**7**] Silicon NPs (Si NPs) are used for photodynamic therapy of cancer employing $^1O_2$ to kill cancer cells,[**34**] Si NPs generate $^1O_2$ after excited by 514.5 nm laser light.[**35,36**] Surface functionalization of NPs with various moieties such as amines/azides (NH_3/N_3) can yield ROS even without any light irradiation.[**37-41**] The ROS generation from Si NP may be possible at lower wavelength of photon after suitable surface modification. In this regards 2-methyl 2-propenoic acid methyl ester [$Si_3O_6(C_5O_2H_8)$] modified Si NPs (Si-MMA) with sizes of ~3±1 nm efficiently generated $^1O_2$ after irradiation with 300-400 nm light due to energy transfer from its exciton singlet state to O_2 and having an exciton triplet with <0.98eV.[**34**]The environmental conditions of ROS generation from metallic NPs can also be varied according to the variation in metal as well as particle size, surface modifications. In this respect, uncoated silver NPs (Ag NPs) having particle sizes of ~5-10 nm can produce primary ROS even in the dark[**42**] whereas PVP and hydrocarbon coated Ag NPs with larger particle sizes of ~30-50 nm can produce ROS in room light (energy density of 6.3J/cm^2).[**43,44**] Choi *et. al.* had investigated the generation of ROS in PVA coated Ag NPs with sizes 9-21 nm) under natural light but the ROS yield was reduced with the increased concentration of Ag NPs due to reduction of the specific surface area.[**45**] Surface capping fundamentally prevents aggregation and provides shielding, which in effect requires more photon energy to release electrons from the surface of Ag NPs.[**46, 47**] Apart from photometric conditions, the selective generation of ROS also depends on surface coating of Ag NPs, for example, PVP coated Ag NPs would not yield $O_2^{\cdot -}$, whereas citrate coated Ag NPs yields higher amount of $O_2^{\cdot -}$ than bare Ag NPs under UV-365 light illumination as PVP coating acts as shield for electron donor and acceptor sites of Ag NPs, and bare Ag NPs produced higher Ag^+ that consumes $O_2^{\cdot -}$through photo-oxidation. No detectable signature of $^{\cdot}OH$ and $^1O_2$ were obtained from citrate and PVP capped Ag NPs when exposed to UV of 365nm [**48**] Liu *et. al.* had reported production of H_2O_2 from citrate capped Ag NP that further stress on generation of $O_2^{\cdot -}$ from the particular NP.[**49**] ROS

production from citrate capped Ag NPs was further evident from Bastose's investigation. Citrate capped spherical Ag NPs (size of 27.1 nm) exhibited intracellular ROS mediated apoptosis of human keratinocyte cell line (HaCaT) and assisted DNA damage at higher extents due to the negatively charged surface. [**50**] $^1O_2$ generation may not be possible in Ag NP due to inability to produce holes under light stimulation. In the case of Au NPs (Au NPs), the shape and capping play vital roles in defining their cytotoxicity. When Au NPs were capped with triphenylphosphine sulfonate (TPPMS), the NPs with sizes of ~ 1.4 nm produced ample amounts of intracellular ROS in Hela cell to cause morphological changes (rounding up the cells) and leakage of mitochondrial constituents, whereas those with sizes of ~ 15 nm did not. Interestingly, Au NPs capped with glutathione (GSH) with sizes of ~1.1 nm produced less ROS.[**51**] This interesting observation supports smooth penetration of smaller sized particle in the cell and the cell morbidity dependence on capping agent. GSH is a well-known natural ROS scavenger in mammalian cell whose depletion encourages ROS production.[**52**] Therefore, GSH capped AuNPs inhibited further yield of ROS. TPPMS coated Au NPs with particle sizes of ~5-250 nm produced $O_2^{\cdot -}$ in DI water after UV irradiation, whereas citrate based Au NPs with similar size ranges yielded $O_2^{\cdot -}$,$^{\cdot}OH$ and $^1O_2$ after X-ray irradiation.[**53**] This diverse observation may be attributed to the surface charge of the coated NP. Au and Ag NPs (size of 30 nm) were also shown to exhibit in vivo ROS mediated cytotoxicity in a model organism (zebrafish). The dissected Ag and Au treated gill, liver tissues demonstrated greater levels of intracellular ROS mediated toxicity for Ag NPs than Au NPs.[**54**] Citrate capped Au NPs with sizes of ca. 15 nm had deleterious effects such as decreased life span and fertility to *Drosophila* flies because of the generation of elevated intracellular ROS and DNA damage.[**55**] The same composition with sizes of ~ 5-20 nm produced ROS in rainbow trout hepatocytes in the dark.[**56**] This may be attributed to quick penetration of the NP into the cell and elevated generation of ROS due to smaller size and higher specific surface area. Flavonoid capped Au NPs with sizes of ~25-30 nm produced ROS in PBS and bare Au NPs in room light produced intracellular ROS in *E.coli* cell causing cytotoxicity (MBC/MIC ratio is 4 and inhibited tRNA) function.[**57,58**] Nickel NPs (Ni NPs) with sizes of ~20 nm induced $^{\cdot}OH$ mediated cytotoxicity in rat macrophages resulting in 50% depletion of supercoiled DNA,[**59**] whereas Cobalt NPs(Co NPs) with sizes of ~ 28 nm size induced cytotoxicity in human endothelial cells (40% cell reduction) by intracellular ROS but with higher particle sizes (of<100 nm) produced ROS in PBS buffer after irradiation by 365 nm light.[**59**] Although the underlying mechanism is not explored but there is ample opportunity to investigate such mechanism to devise future nanomedicine. Mohamed *et. al.* had reported the ROS induced antibacterial effect of Au NPs (25nm) against *corynebacterium pseudotuberculosis* via formation of vacuoles.[**60**] There exists another report supporting non-photometric ROS generation from metallic nanoparticles, e.g., copper nanoparticles modified by Mercaptooctanoic acid with variable chain length exhibited distinguishable H_2O_2generation in dark.[**61**] Ahmad *et.al.* investigated that chitosan coated Ag NPs (size of 15-25 nm) exhibited higher intracellular ROS generation than uncoated NPs which would lead to improved antibacterial activity in the dark.[**62**]Also the surface modification by chitosan molecule promotes Ag NPs more cationic in nature which facilitates higher antibacterial activity against both gram positive and gram negative bacteria.[**62**] This implies larger particles which resembles bulk structures yield ROS after light irradiation, whereas lower sizes can produce extra/intracellular ROS even in dark conditions.[**63,64**] Excluding the effect of surface coating and quantum confinement, uncoated Au, Ag, Si and Ni NPs having size ranges of ~ 20-30 nm exhibited different types of ROS generation with quantified amounts under 365 nm irradiation;[**7**] Ag NPs were observed to selectively produce $O_2^{\cdot -}$ and $^{\cdot}OH$, whereas Au, Si and Ni NPs effectively produced $^1O_2$ with maximum yield for Si NPs.

Non-Metallic NPs

Non-metallic NPs are also interesting for a variety of biological applications Bare Polystyrene NPs could not yield ROS in phosphate buffer (PBS) under UV-365 nm irradiation as Polystyrene is neither semiconductor nor photosensitizer but the same NPs with sizes of ~600 nm after surface modification with NH_2 yielded intracellular ROS in RAW 264.7 macrophages under the same stimulation, whereas the surface modification with COOH functionalization did not produce any ROS under 365 nm irradiation. This may be due to anionic surface charge (zeta potential for bare polystyrene is -36.4 mV , COOH-Polystyrene is -27.6 mV and NH_2-Polystyrene is 45.8mV).[**65**]Anionic surface of polystyrene (COOH-Polystyrene) has a lower ROS generation due to significant repulsion of the particle with anionic lysosomal cell resulting lower cytotoxicity [**65**] Fullerene (C_{60}) produced primary ROS in DI water, PBS and human keratinocyte cells in visible light due to conversion of triplet state $^3C^*_{60}$ into $C_{60}^{\cdot-}$ which subsequently reduces molecular oxygen to $O_2^{\cdot-}$ that further transforms into $^{\cdot}OH$.[**66,67**] After surface modification with ozone, C_{60} produced $O_2^{\cdot-}$, $^1O_2$ and $^{\cdot}OH$ after 365 nm illumination,[**68**] whereas PVP coated C_{60} produced only $O_2^{\cdot-}$, $^1O_2$ after 365nm illumination due to development of more acidic pH (~4) that encourages electron transfer between $^{\cdot}OH$ to $O_2^{\cdot-}$.[**69,70**] as described in the following equations:

$$\cdot OH + O_2^{\cdot-} \rightarrow 1O_2 + OH^- \quad (7)$$

$$2H^+ + 2O_2^{\cdot-} \rightarrow 1O_2 + H_2O_2 \quad (8)$$

CdTe QDs which are visible light driven semiconductors imparted oxidative stress onto bacteria by inducing $O_2^{\cdot-}$ after excitation with 440 nm light,[**71**] whereas after coating with MPA the same CdTe QDs were able to produce the most damaging ROS (i.e.,$^1O_2$) in vitro after excitation by 488 nm light. InP/ZnS QDs (sizes of ~ 2.8 nm) produced extracellular $^{\cdot}OH$ and $O_2^{\cdot-}$ after excitation at 400 nm visible light.[**2**] Biotin conjugated CdSe/ZnS produced $^{\cdot}OH$ and $O_2^{\cdot-}$ after exciting with solar radiation (λ=290-400 nm).[**72**] Very few reports exist on ROS generation from polymer-based materials.

Metal Oxide NPs

Metal Oxide NPs can also produce ROS under different environmental conditions according [**69, 73-75**] but there exists some ambiguity regarding ROS generation by metal oxides; reports of ROS production by TiO_2in the dark is not consistent, likewise for nTiO_2production of $O_2^{\cdot-}$ in *E.coli*.[**10,64,69,75**] Interestingly nCeO_2(ca. 8 nm) suppressed ROS production in RAW 264. 7 and BEAS- 2B cells thus protecting the cells from oxidative damage,[**76,77**] whereas another study found nCeO_2 inhibited *E.coli* growth by pumping oxidative stress;[**78**] nCeO_2 (ca. 20 nm in diameter) promoted toxicity in BEAS-2B lung cells for which an incremental ROS level was developed with the subsequent decrease in glutathione level which further increased malondialdehydes.**[79]** ROS production by metal oxides is largely dependent on the specific environmental conditions: illumination intensity, illumination conditions, particle sizes, concentrations, pH and redox chemistry of the solution etc., and meaningfully comparable data requires validated studies of the ROS production from all metal oxide NPs under same experimental conditions. Li *et. al.* studied different types of ROS generation from nTiO_2, nZnO, nSiO_2, nCeO_2, nAl_2O_3, nCuO under 365nm irradiation, where n represents the donor type semiconducting nature of the materials.[**10**] Among metal oxide NPs, nCuO NPs did not produce any ROS, whereas maximum generation was observed for nTiO_2. The total ROS generation paradigm is as follows:

$nTiO_2$>$nZnO$> nAl_2O_3> $nSiO_2$> nFe_2O_3> $nCeO_2$ > nCuO.[**10**] Among three types of ROS ($^{\cdot}OH$, $O_2^{\cdot-}$, $^1O_2$), $O_2^{\cdot-}$ is mostly generated in nZnO NPs followed by nFe_2O_3, $nTiO_2$ and $nCeO_2$. nAl_2O_3, $nSiO_2$ and nCuO could not generate $O_2^{\cdot-}$.[**10**] Conversely $nTiO_2$ exhibited highest production of •OH even 2-fold and 6-fold higher than nZnO and nFe_2O_3.[**10**] In the case of SiO_2, significant amounts of $^{\cdot}OH$ radicals are generated, as reported by Yu *et. al.* [**80**] They had showed size-dependent $^{\cdot}OH$ production from SiO_2 NPs. Lowering the size resulted in higher yields of $^{\cdot}OH$ radical in both in-vitro and in-vivo studies [**80**] Lehman *et.al.* also reported the recognizable production of $^{\cdot}OH$ radical from SiO_2 NPs where the surface area and surface charge play key role in defining the yield of $^{\cdot}OH$ radicals. [**81**] Thomassen *et. al.* had also investigated the production of $^{\cdot}OH$ radicals from amorphous SiO_2 NPs (size range is of 2-335 nm) and there was a substantial increase in $^{\cdot}OH$ radical in a time-dependent fashion. The $^{\cdot}OH$ yield was found to be dependent on synthesis route, particle size, etc.[**82**]

In the case of $^1O_2$ generation $nTiO_2$ gives out highest efficiency compared to nAl_2O_3 followed by nZnO and $nSiO_2$.[**10**] Such difference is likely to occur due to variation in defect properties, structural disorders and most importantly electronic structures. Apart from photon energy stimulation, size-dependent ROS generation and phototoxicity of TiO_2 (<25 nm, 31 nm, <100 nm and 325 nm) was reported by Yin *et. al.* where higher ROS production was observed for smaller sized particle due to enhanced surface area.[**83**] Size- and dose-dependent ROS production and cytotoxicity were also reported by Chen *et. al.* where the ROS production was gradually increased with increasing quantities of ZnO NPs (0-6 mg/L) but decreasing particle sizes (20 nm > 90 nm> 200 nm). The ROS-induced cell toxicity for these ZnO NPs was assured with the help of cellular GSH variation at similar rhythm. [**84**] Genotoxicity is considered as an outcome of ROS-induced oxidative stress [**85**] and Peterson *et. al.* had reported DNA damage by TiO_2 nanoparticles at a variety of illuminations, i.e., dark, visible light and UVA light. For UVA light irradiation, low concentrations of TiO_2 nanoparticles can cause oxidative stress on DNA as compared to visible light condition, whereas no DNA damage was observed in the dark due to its bandgap energy.[**86**] Dependence of the ROS generation from nanosized ZnO on illumination time and wavelength were reported by Lipovsky *et. al.* The $^{\cdot}OH$ production was primarily increased with the illumination time and reaches plateau due to recombination of ROS. The intensity of $^{\cdot}OH$ radicals was higher with blue light illumination as compared to white and red light due to enhanced electron-hole pair generation.[**87**] Morphology-driven ROS generation from MgO nanoparticles was observed by Podder *et. al.* MgO nanorods produced higher $O_2^{\cdot-}$ as compared to MgO nanoparticles and nanoplates in the dark due to the evolution of F_2^{3+}, F_2^{+}, and F^{+} states and $^{\bullet}OH$ was yielded via an $O_2^{\cdot-}$ mediated pathway [**29**]. pH stimulated ROS generation and resultant oxidative stress on bacterial population was observed in nano CeO_2 (size of 3-4 nm).[**88**] The intracellular ROS was elevated at pH 9, whereas no trace of ROS was obtained at pH 6 which also correlated the higher antibacterial efficacy at pH 9 environment. At higher pH the surface charge of CeO_2 was positive (11.76±3.54mV) that facilitated enhanced antibacterial activity and ROS production. The ROS yield was subjected to the appearance of higher Ce^{4+} states (lower Ce^{3+}/Ce^{4+} ratio that indicates catalytic property)[**88**] Nano CeO_2 also showed pH-dependent cytotoxicity on bone cancer cells (osteosarcoma cells) where cell viability was highly reduced at pH 6 (acidic environment) as compared to pH 7 and pH 9 (physiological and basic environment)[**89**] The ROS-induced cytotoxicity of CeO_2 is developed towards cancer cell at acidic environment due to transformation of Ce^{3+} to Ce^{4+} states that facilitates its catalytic activity.[**90,91,89,92**] pH-dependent ROS generation was recently observed by Dutta *et. al.* who had studied the effect of pH on toxicity of CeO_2 NPs. When the NPs was synthesized at alkaline pH there was no

toxicity effect on zebrafish larvae but the same NPs synthesized at acidic pH was found to be cytotoxic and genotoxic on the larvae [**93**]

Relation of ROS Generation with Electronic Structure of Nanomaterials

ROS generation profiles of different nanomaterials varies due to their electronic structures and redox states under similar experimental conditions.[**7**] The general mechanism behind redox controlled ROS generation is as follows: the redox couple (E_H) of $O_2/O_2^{\cdot-}$ is -0.2 eV[**7**] and from eq (1) as it is a conduction electron mediated process, so the band edge potential of the conduction band (E_{CB}) will be less than -0.2eV for detectable $O_2^{\cdot-}$.[**7**] Similarly the E_H of $H_2O/{}^{\cdot}OH$ is 2.2 eV, and as it is related to valence band (hole enriched energy state) according to eq (5), the band edge potential of valence band (E_{VB}) should be greater than 2.2eV[**7**] for successful generation of ${}^{\cdot}OH$. Concomitantly, the E_H of $O_2/{}^1O_2$ is 1.88eV and according to eq (6) this valence band centered $^1O_2$ conversion requires: E_{VB}> 1.88eV for potential production of $^1O_2$.[**7**] Thus depending on the redox potential of energy state, nanomaterials selectively produce ROS under identical environmental conditions.

Metallic NPs

The most commonly used metallic NPs (Si, Ag, Au, Ni) are highlighted here due to their frequent use in industrial/commercial, and biomedical fields, and to correlate their antibacterial properties essential for environmental purposes.[**34,94-96**] Si NPs have a band gap of 2.0 eV with E_{CB} and E_{VB} of 0.1 and 2.1 eV, respectively,[**97**] so it cannot produce ${}^{\cdot}OH$ as well as $O_2^{\cdot-}$ as explained previously, and as aforementioned $^1O_2$ generation is possible. The theme of different ROS generation is demonstrated in **Figure 1.**

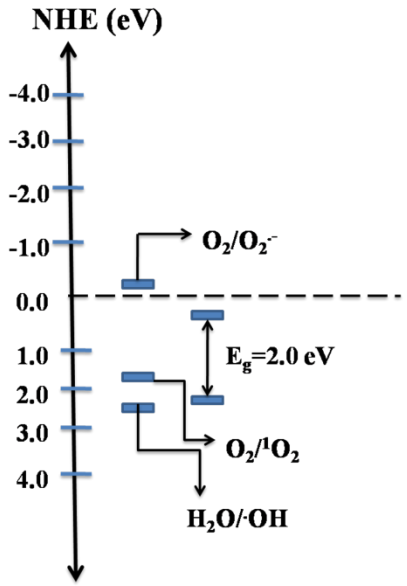

Figure1. Band edge positions of Si NPs in aqueous suspension (pH 5.6) demonstrating band gap (E_g) = 2.0 eV and also the positions of different redox couple illustrating selective generation of ROS. All measurement was carried out with respect to normal hydrogen electrode (NHE).[**7**]

Ag and Au NPs being noble metals display the surface plasmon resonance (SPR) effect (i.e., coherency between surface electron oscillating frequency with UV light frequency, in cases

where the wavelength of UV radiation >> size of NPs). This SPR effect transfers energy from molecular oxygen to singlet oxygen,[**7**] and the energy transfer causes production of $O_2^{\cdot-}$ which produces more $^{\cdot}OH$.[**7**] Thus Ag and Au NPs produce $^1O_2$, $O_2^{\cdot-}$ and $^{\cdot}OH$.[**7**] Ni NPs have large optical absorptions which reduces the SPR effect, thus $^1O_2$ generation is low.[**7**]There is also ambiguity regarding Ag NPs producing $O_2^{\cdot-}$ and $^{\cdot}OH$ but no detectable amounts of $^1O_2$.[**7**] This may be due to photocorrosion of Ag NPs which is essentially the alteration of redox chemistry of the Ag NP solution after exposure to UV light and concomitant evolution of the redox couple Ag^+/Ag.[**7**]The aggregation of NPs or increase in hydrodynamic size reduces production of ROS (Ni NPs display similar behavior).[**7**]

Properties of Metal oxide NPs

The properties of metal oxide NPs (low cost, non-toxicity, high chemical stability, high redox potential) [**98**] can offer potential for biomedical applications including: antibacterial activity, sunscreen lotion, wound healing, anticancer therapy (due to their photocatalysis for ROS generation).[**99-101**] ZnO and TiO_2 are extensively used in biomedicine due to their high performance in ROS generation, and other metal oxides are being developed for biomedical applications. Evaluation of E_{CB} and E_{VB} of metal oxide NPs is possible using Mulliken's electronegativity and E_g [**102**] as these band edge potentials are necessary to understand charge transfer, ROS generation (which is dependent on redox potentials of ROS generation reactions)[**103,104**] and antibacterial activity.[**105**]The values of E_{VB} and E_{CB} are derived as follows:

$$E_{VB}=\chi - 4.5 + \frac{1}{2} \times E_g \quad (9)$$

$$E_{CB} = E_{VB} - E_g \quad (10)$$

Where χ is Mulliken's electronegativity, the geometric mean of absolute electronegativity of constituent elements. E_g is the band gap of metal oxide NPs (derived from Wood-Tauc's plots)

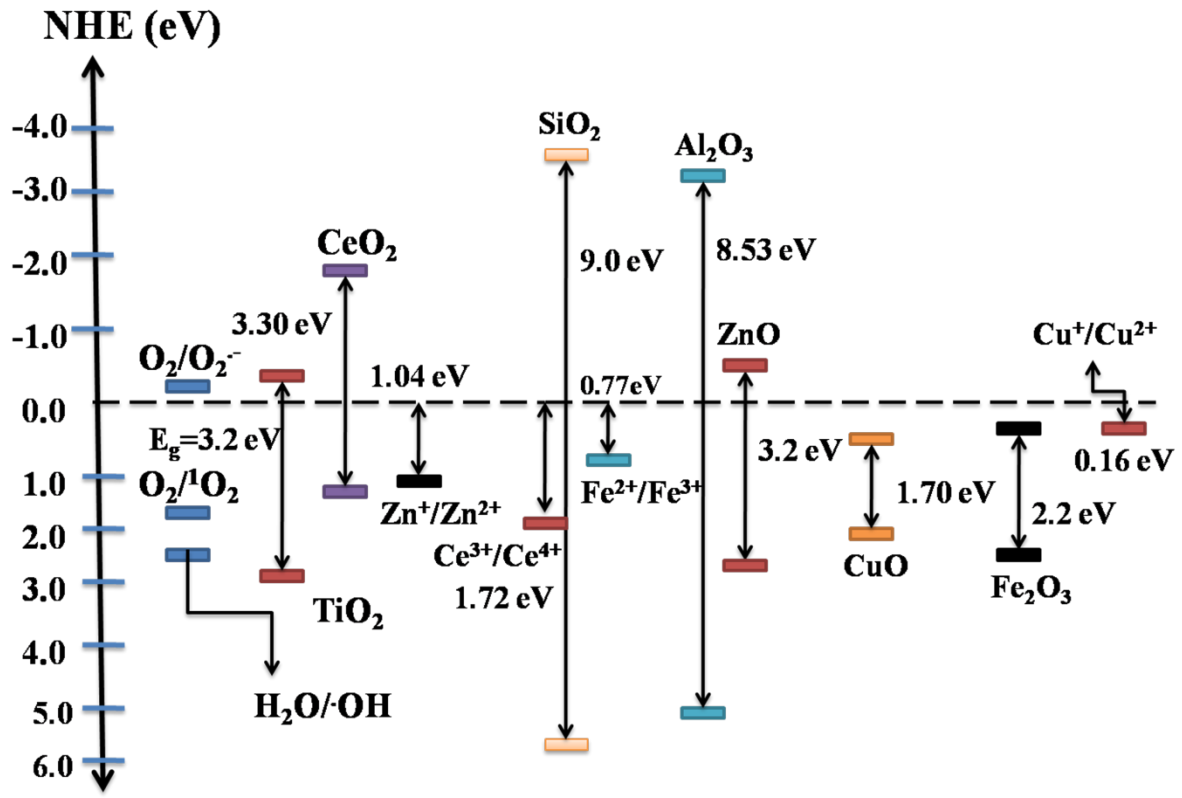

Figure 2. Band edge potentials of different metal oxides along with free radicals and ionic species in NHE scale.

Butler *et al*. had proposed an empirical relationship of E_{CB} and E_{VB} with the pH of photochemical reactions, [**106**] wherein the band edge energies shift lower/higher energy depending on space charge layer and electrostatic double layer (Helmholtz layer) which are formed at the interface between the metal oxide and aqueous solution.[**103,107**] If the pH of the photochemical reactions is 5.6,at this pH value E_{CB} and E_{VB} are calculated as follows: [**106**]

$$E_{\{CB|5.6\}} = E_{CB} + 0.059 \times (PZZP - 5.6) \quad (10)$$

$$E_{\{VB|5.6\}} = E_{VB} + 0.059 \times (PZZP - 5.6) \quad (11)$$

Where PZZP is the point of zero zeta potential of a semiconductor.E_{CB} for $nTiO_2$ and $nCeO_2$ as reported by Li *et al*. were -0.28 and -1.69eV at pH 5.6, respectively, whereas that of for nZnO was found to be -0.12eV.[**10**] E_H of $O_2/O_2^{\cdot-}$ is -0.2eV w.r.t. NHE at pH 5.6 so $nTiO_2$ and $nCeO_2$ have the potential to donate electrons to O_2 to generate $O_2^{\cdot-}$, whereas nZnO should not produce $O_2^{\cdot-}$ because ECB > E_H of $O_2/O_2^{\cdot-}$.However, it was found experimentally that nZnO has the highest ability to produce $O_2^{\cdot-}$ due to its n-type semiconducting nature, and at the interface of aqueous solution there is an upward bending of the conduction band due to accumulation of positive charges, as a result of which the actual value of E_{CB} could be lower than that of E_{CB} at pH~5.6.[**108**] nAl_2O_3 and $nSiO_2$ possess higher band gaps (>365nm) so they could not donate photoexcited electrons from the conduction band to molecular oxygen. nFe_2O_3 due to its higher E_{CB} (0.46eV) would not normally donate electrons to form $O_2^{\cdot-}$, but

due to n-type behavior it can do the same as nZnO. nCuO does not produce $O_2^{\cdot-}$ due to its higher E_{CB} (0.69eV).[**10**]

Interestingly these oxide materials can produce $^{\cdot}OH$ (E_H of $H_2O/^{\cdot}OH$ =2.2 eV) in measurable quantities due to their higher E_{VB} (2.92eV for $nTiO_2$, 3.08eV for nZnO, 2.39eV for nCuO, 2.66eV for nFe_2O_3), but experimentally nCuO does not generate $^{\cdot}OH$ which may be due to small differences between the E_{VB} of nCuO and E_H of $H_2O/^{\cdot}OH$. [**10**] Similarly all metal oxides except $nCeO_2$ (E_{VB}=1.6eV), Al_2O_3 and SiO_2 generate $^1O_2$ (E_H of $^1O_2/O_2$=1.88eV) as reported Li *et. al*.[**10**] Their group also reported nCuO and $nFe_2O_3$to be ineffective for $^1O_2$ generation although their E_{VB} = 2.16 and 2.48 eV, [**10**] this is due to the rapid consumption of produced $^1O_2$ by Cu^+ and Fe^{2+} ions formed after their conversion from Cu^{2+} and Fe^{3+} due to the lower potential of the redox couples Cu^+/Cu^{2+} (E_H=0.16eV) and Fe^{2+}/Fe^{3+} (E_H=0.77eV). For ZnO this situation did not occur as the E_H of Zn^+/Zn^{2+}= 1.04eV.[**10**] nAl_2O_3 (E_g= 8.53eV)[**10**] and $nSiO_2$ (E_g=9.0 eV)[**10**] did not produce any trace amount of $^{\cdot}OH$ as well as $^1O_2$ due to their large band gap. The aforementioned observations require UV light irradiation (λ=365 nm) factors; room light (intensity~10 μW/cm^{-2}) induces ROS generation from ZnO.[**109**]Visible light (blue light, λ=400-500 nm) promotes generation of $^{\cdot}OH$ and $^1O_2$ from ZnO suspensions as demonstrated by EPR spectroscopy.[**110**] Interestingly metal oxide NPs (e.g., ZnO) may generate $^{\cdot}OH$ in the dark (no specificity of light condition) as demonstrated by EPR spectroscopy,[**110,111**] there are also numerous reports of the antibacterial activity of metal oxides in the dark, although the intensity is lower than in the presence of light.[**3,112,113**] Xu *et al.* demonstrated H_2O_2 generation from ZnO nanostructures in the dark imparts antibacterial activity, and oxygen vacancies (V_o) are a significant factor for the generation of H_2O_2.[**114**] Prasanna *et al*. had also reported three types of ROS ($O_2^{\cdot-}$, $^{\cdot}OH$, H_2O_2) generated from nZnO in the dark, and observed $O_2^{\cdot-}$ mediated antibacterial activity; they also demonstrated that the presence of singly charged oxygen vacancy (Vo^+) by EPR and scavenging studies was responsible for $O_2^{\cdot-}$ generation.[**5**] Okays *et al.* showed that it was possible to generate ROS from ZnO nanorods using glutathione (g-l-glutamyl-l-cysteinyl-glycine, GSH) oxidation in the dark. [**115**] GSH, present in all prokaryotic and eukaryotic cells, protects the cells from oxidative stress induced by ROS, so oxidation of GSH becomes an indirect method to quantify ROS generation.[**115**] Ghosh *et al*. had detected $^{\cdot}OH$ from ZnO and ZnO/chitosan NPs in the dark via EPR and $^{\cdot}OH$ were proven to be responsible for killing *S.aureus*.[**116**] It is noteworthy that ROS generation in the dark, and the mechanism underpinning it for a variety of nanomaterials is still under research.

ROS Mediated Antibacterial Activity of Metal oxide Nanostructures and Their Composites

ZnO is a particularly well-known example of an antibacterial metal oxide. Being an n-type semiconducting metal oxide it has various levels of oxygen vacancies [**117**] which essentially act as electron donor sites and facilitate the generation of $O_2^{\cdot-}$ and related ROS,[**5,114**] that underpin the antibacterial activity of ZnO and its hybrid structures.[**116,118**] Zn^{2+} ion employed in wound healing due to its anti-inflammatory, drying, antiseptic and astringent properties.[**119**] Most of the research on ZnO has focused on the study of effect of variation in morphology, shape, size, synthesis parameters etc., on antibacterial activity.[**120-123**] Our current mechanistic understanding of the antibacterial activity of ZnO nanostructures is based on Zn^{2+} ion dissolution and internalization of nanostructures which eventually results in death of the bacteria due to consumption of excessive Zn^{2+} ions and physical damage of bacterial cell membranes.[**118, 124**] Singh *et al.* proposed that the morphology of nanomaterials plays a role in their antibacterial activity,[**125**] designing ZnO spheres, nanorods, cauliflowers and

mushroom-like architectures to study their antibacterial activity against *S. aureus* under UV light and in the dark. The antibacterial activity was particularly high for the cauliflower-like structures, and higher under UV light than in the dark; and such activity was ascribed to be due to the presence of a large number of oxygen vacancies (evidenced by photoluminescence spectroscopy) and that these native point defects produced enhanced ROS production when exposed to UV light.**[125]** ZnO based composite materials (e.g., Ag-ZnO/Chitosan complexes, Polyaniline/Cu $_{0.05}Zn_{0.95}O$ complexes, Graphene oxide/ZnO) illustrate the potential of such materials to display antibacterial/antifungal activity.[**126,127,128**] In addition to ZnO nanostructures, other metal oxides (e.g., TiO_2, Fe_2O_3,Fe_3O_4, CuO, MgO etc.) show antibacterial activities, the mechanism of antibacterial activity typically ascribed to ROS production under various environmental condition (e.g., UV-Vis exposure, in the dark, etc.).[**129-138**] Raut *et al.* reported that the mechanism of antibacterial activity of nitrogen doped $TiO_2$was related to native point defects (oxygen vacancies measured by X-ray photoelectron spectroscopy) and ROS production under UV (380 nm), sunlight and room light; the excellent bactericidal properties of nitrogen doped TiO_2 under room light and sun light was observed to be due to increased charge carrier separation (**Figure 3**) owing to oxygen vacancies which facilitate disruption of cell membranes by ROS, disordering of inner cytoplasmic membranes and decomposition of bacterial cells (however, no direct evidence of ROS production was reported).[**129**] Similar charge carrier separation induced high bacterial (*S. aureus*) inactivation by carbon doped anatase-brookite TiO_2 nanoheterojunctions, wherein charge carrier separation enhances ROS generation and thereby antibacterial activity.[**98**] This visible light induced antibacterial activity could be extended to the dark after conjugation of silver halide/TiO_2 with hydroxyapatite.[**139**] The phosphate (PO_4^{3-}) group under UV illumination acts as an electron trapping centre due to formation of oxygen vacancies which facilitate generation of $O_2^{\cdot -}$, and in the dark there are covalent bonds formed between bacterial surfaces and PO_4^{3-} groups which interfere with bacterial nutrient uptake from the environment which inhibit bacterial growth instead of killing bacteria.[**139**]

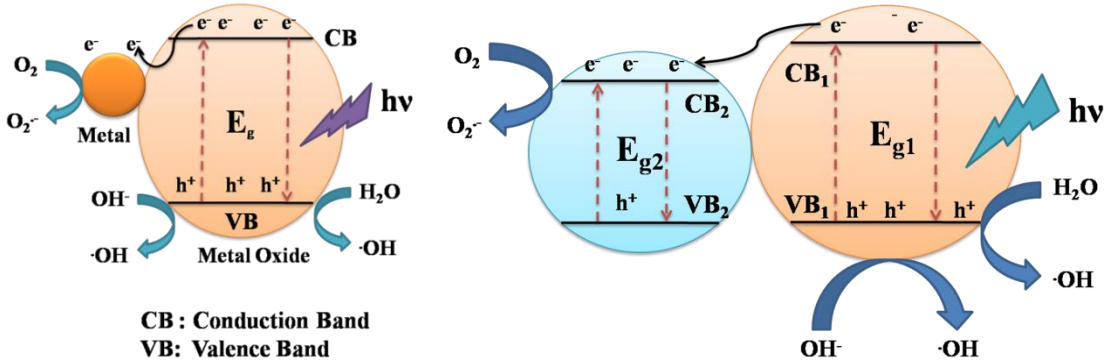

Figure 3. ROS generation due to charge carrier separation in (left) metal-metal oxide nanoheterojunction and (right) semiconductor-metal oxide nanoheterostructure.

Similar dark and visible light induced antibacterial activity of $CuO/Cu(OH)_2$ hierarchical structures was documented by Akhvan *et. al.*, where visible light driven antibacterial activity is attributed to ·OH radical generation from adsorbed -OH species on CuO surfaces due to reaction with photogenerated holes, whereas in the dark the antibacterial behavior was due to increased Cu^{2+} ion release from higher surface density and physical damage of cell membranes.[**135**] The correlation of ROS generation (experimentally) with antibacterial activity in different light conditions is highlighted in **Table 1**.

Table1.Examples of metal NPs with their ROS generation capability and correlation with antibacterial activity in both light and dark conditions (the antibacterial mechanism of metallic NPs are based on non-ROS mediated processes).

Metal oxides	Morphology	Source	Experimental conditions of ROS generation	ROS generation methods	ROS produced	Antibacterial activity	Mechanism of antibacterial activity	Ref
ZnO	Nanorod	Sonochemical	Dark,2 h incubation	GSH oxidation	H_2O_2	*B. subtilis*-100% *E. coli*-95% (2 h exposure)	H_2O_2 induced	**115**
ZnO	Bare NPs, Oxalic acid capped NPs	Wet chemical	Dark	$KMnO_4$ titration, Fluorescence spectroscopy (FL)using Terephthalic acid (TA), NBT degradation, EPR using DMPO	$O_2^{\cdot-}$,·OH, H_2O_2	*S. aureus* - 17% *E. coli* - 25% in the dark	$O_2^{\cdot-}$ mediated and singly ionized oxygen vacancy (EPR and PL measurement) controlled	**5**
ZnO	Tetra pod, NPs, micron sized	Gas expanding method, Commercial	Dark and solar light (150W Xenon lamp)	EPR using DMPO, FL spectroscopy using TA, KI and Starch method	H_2O_2 under dark and ·OH under light	*E. coli* - 76% for tetra pod,65% for NPs,60% for micron sized	H_2O_2 induced and Oxygen vacancy (EPR and XPS measurement) mediated	**114**
ZnO	NPs	Commercial	UV, 365 nm light (2 h irradiation)	UV-Vis spectroscopy using XTT, p-Chloroben	$O_2^{\cdot-}$, ·OH, $^1O_2$	*E. coli*-survival rate=Log(N_t/N_0)= -	$O_2^{\cdot-}$ mediated	**10**

				zoic acid, FFA		0.5		
CuO	NPs	Commercial	UV-365 nm light (2 h inrradiation)	UV-Vis spectroscopy using XTT, p-Chlorobenzoic acid, FFA	No ROS produced	*E. coli*-survival rate=Log(N_t/N_0)= -0.9	High Cu^{2+} mediated antibacterial activity	**10**
CeO_2	NPs	Commercial	UV-365 nm light (2 h irradiation)	UV-Vis spectroscopy using XTT, p-Chlorobenzoic acid, FFA	$O_2^{\cdot -}$	Almost no antibacterial activity	Shield for E.coli and scavenges ROS	**10**
SiO_2	NPs	Commercial	UV-365 nm light (2 h irradiation)	UV-Vis spectroscopy using XTT, p-Chlorobenzoic acid, FFA	$^1O_2$	*E. coli*-survival rate=Log(N_t/N_0)= -0.2	$^1O_2$ mediated bacterial death	**10**
Al_2O_3	NPs	Commercial	UV-365 nm light (2 h irradiation)	UV-Vis spectroscopy using XTT, p-Chlorobenzoic acid, FFA	$^1O_2$	*E. coli*-survival rate=Log(N_t/N_0)= -0.3	$^1O_2$ mediated bacterial death	**10**
Fe_2O_3	NPs	Commercial	UV-365 nm light (2 h irradiation)	UV-Vis spectroscopy using XTT, p-Chlorobenzoic acid, FFA	$O_2^{\cdot -}$, $^{\cdot}OH$	*E. coli*-survival rate=Log(N_t/N_0)= -0.1	ROS mediated antibacterial actitvity	**10**
TiO_2	NPs	Commercial	UV-365 nm light (2 h irradiation)	UV-Vis spectroscopy using XTT, p-Chlorobenzoic acid, FFA	$^1O_2$, $^{\cdot}OH$, $O_2^{\cdot -}$	*E. coli*-survival rate=Log(N_t/N_0)= -0.7	$^1O_2$ and $^{\cdot}OH$ mediated antibacterial activity	**10**

ZnO	NPs	Sonochemical	NA	EPR using DMPO, DCFA-H_2 assay	No $\cdot OH$ and very low H_2O_2	*S. mutans* biofilm-85%	Not understood	**140**
CuO	NPs	Sonochemical	NA	EPR using DMPO, DCFA-H_2 assay	No $\cdot OH$ and very low H_2O_2	*S. mutans* biofilm-70%	Not understood	**140**
ZnO	NPs	Commercial	UV 365 nm light (4 h exposure), Dark	UV-Vis spectroscopy using XTT, p-Chlorobenzoic acid, FFA	$O_2^{\cdot -}$, $\cdot OH$, $^1O_2$ under UV -365 nm light, Zn^{2+} in the dark	*E. coli*-100% in DI water	Linear relationship between total ROS and antibacterial activity	**3**
ZnO-Ag	Nanohybrid	Lab synthesized	NA	EPR using DMPO	$\cdot OH$	*E. coli* (MIC)-12 µg/ml; *S.aureus* (MIC)-07µg/ml	Physical attack on cell wall	**116**
ZnO-Au	Nanohybrid	Photoreduction	Solar simulator, 450 W Xenon lamp, Dark	EPR using BMPO, 4-oxo-TEMP, CPH, TEMPO, scavengers e.g., DMSO, SOD, NaN_3	$\cdot OH$ and $^1O_2$	*E. coli*-5% *S. aureus*-10%	ROS induced antibacterial activity and enhancement in ROS is due to enhanced charge carrier reactivity due to electron transfer and	**141**

							charge separation	
TiO_2-Ag	Nanocomposite	Sonochemical	Dark	In-vitro: EPR using DMPO In-vivo: antioxidants, e.g., Superoxide dismutase (SOD) [$O_2^{\cdot-}$ scavenger] Histidine [$^{\cdot}OH$ and $^1O_2$ scavenger]	Negligible in vitro ROS Intracellular ROS of *E. coli*	*E. coli*-Log-Fold reduction = 3.2-4.2	Intracellular ROS ,presence of Ag^+ ion on surface of composite	**142**
GO@CS/ZnO	Nanocomposite	In-situ mixing	Not mentioned	Intracellular ROS using $DCFH_2$-DA, NO detection assay, Catalase activity assay	$O_2^{\cdot-}$	MIC for *E. coli*-2.5µg/ml *S. aureus*-5µg/ml	Attack of $O_2^{\cdot-}$ on carbonyl group of bacterial cell wall leading to protein damage	**143**
ZnO@CS	Nanocomposite	Direct mixing	Dark	In-vitro: UV-Vis spectroscopy using Nitroblue Tetrazolium chloride, Fluorescence spectroscopy using Terephthalic acid	$O_2^{\cdot-}$, $^{\cdot}OH$	MIC for *P. putida*-5µg/ml	Massive generation of .OH from the composite (ZnO:CS =2:1) due to strong interfacial interaction and develop	**4**

							ment of rich acceptor level in the composite for generation of holes in the dark	
Ag_3PO_4 @P-olyindole	Nanocomposite	In –situ mixing	Dark	Intracellular ROS measured by DCFH-DA fluorescence assay and Membrane disintegrity test using Propidium Iodide	H_2O_2	MIC for *E. coli*- 0.5µg/ml and *S. aureus*- 5µg/ml	Long term antibacterial activity (7 days) subjected to generation of intracellular H_2O_2	**144**

The Antioxidant Activity of Nanomaterials

Antioxidant activity (i.e., scavenging of free radicals) is important as it diminishes radical mediated oxidation of biomolecules in cells under various conditions (e.g., exposure to cisplatin, diallyl trisulfide, UVA irradiation, lipopolysaccharides, phorbol 12-myristate 13-acetate, high glucose contents, oxidized low density lipoprotein, hypoxia-hypoglycemia and reoxygenation, doxorubicin).[**145**] Nanomaterials (e.g., Prussian blue, Pt, CeO_2, Fe_3O_4 NPs, fullerenes and polymers) have potential applications in inflammatory treatment, cancer cell therapy, tissue engineering, nanomedicine [**145-148**] etc as artificial enzymes (with size-dependent properties, enrichment with surface defects, etc.) and they are preferred over natural extracellular antioxidants viz. Vitamin C, E, coenzyme in regards of higher chemical stability, improved efficacy, satisfactory bioavailability etc. [**23**] Prussian blue NPs (sizes of ~ 50 nm) effectively scavenge H_2O_2,·OH and $O_2^{\cdot-}$ via peroxidase (POD), catalase (CAT) mimetic pathway at low pH, while superoxide dismutase (SOD) activity was observed at different pH values in concentration-dependent manner; further studies revealed that it is a good ·OH scavenger (demonstrated in-vitro using a ROS generating model) and reduced inflammation in macrophages in vitro and in an in vivo mouse model.[**145**] Pt NPs can scavenge superoxide anion radicals ($O_2^{\cdot-}$) and hydroxyl radicals (·OH) [**146**] as demonstrated by the hypoxanthine−xanthine oxidase system (for $O_2^{\cdot-}$) and Fenton analysis and a UV/H_2O_2 system (for ·OH), supported by EPR analysis which revealed that 2 nm NPs potentially scavenged $O_2^{\cdot-}$ and ·OH with rate constant (for the $O_2^{\cdot-}$ scavenging) was $5.03 \pm 0.03 \times 10^7$

M^{-1} s^{-1}. Interestingly Pt NPs with sizes of ~ 1 nm showed the highest $O_2^{\cdot-}$ scavenging activity, however, the ·OH-scavenging reaction remained undetermined in both systems. Pt NPs are non-toxic to a variety of adherent cells (TIG-1, HeLa, HepG2, WI-38, and MRC-5) at concentrations of up to 50 mg/L, and the NPs scavenged intracellular ROS in HeLa cells. Moreover, Pt NPs significantly diminished the levels of intracellular $O_2^{\cdot-}$ generated by UVA irradiation and inhibited ROS damage-induced cell death of HeLa cells.[**146**] Among metal oxide NPs, CeO_2 NPs can be used as radical scavengers to diminish oxidative stress-induced damage (interesting (interesting for neuroprotection, radioprotection and anti-inflammation);[**147, 149-153**] where the radical scavenging in biological systems is due to reversible conversion of the Ce^{3+}/Ce^{4+} redox couple (E_H of Ce^{3+}/Ce^{4+} =1.72 eV). CeO_2 NPs with higher Ce^{3+}/Ce^{4+} ratio (due to oxygen vacancies) showed a higher SOD activity than with lower Ce^{3+}/Ce^{4+} ratio; SOD activity decreases by changing the Ce^{3+}/Ce^{4+} ratio and the scavenging activity can be restored upon reduction of the particles in solution.[**154**] Tain *et al.* studied the effect of surface properties (e.g., surface defects, morphology) using different morphologies of CeO_2(nanorods, porous nanorods and NPs).[**155**] The porous nanorod-CeO_2showed the highest radical scavenging activity measured by a Superoxide dismutase (SOD) assay (the high SOD mimetic activity was caused by high oxygen vacancies (estimated to be 0.52 mmol/g from the concentration of Ce^{3+} active sites) and exposure of (100) crystal facet (observed via TEM). Interestingly, increasing calcinations temperatures that reduced Ce^{3+} concentrations due to decreases in oxygen vacancies (formation of oxygen vacancies in CeO_2 leads to conversion of Ce^{4+}/Ce^{3+} in order to maintain charge neutrality) diminished SOD activity. It is noteworthy that the formation of oxygen vacancy (V^{**}_O) can be described by Kroger-Vink: [**155**]

$$2Ce_{Ce}{}^{4+} + O_O = 2Ce^{3+}{}_{Ce} + V^{++}{}_o + \frac{1}{2}O_2\,(g) \qquad (12)$$

Suspensions (2mg/ml) of porous nanorod-CeO_2inH_2O_2 (50mM) displayed autocatalytic activity ($Ce^{3+}\rightarrow Ce^{4+}$ after immediate exposure and $Ce^{4+}\rightarrow Ce^{3+}$ after 9 days); moreover, such porous nanorods diminished intracellular H_2O_2 in doxorubicin treated H9c2 cells(by 79.5% which was 3.7 times higher than the vitamin E and reduced cell apoptosis by 120% in vitro, and in vivo in a rat model.[**155**] CeO_2 NPs can potentially prevent oxidative stress induced several neurodegenerative diseases (including trauma, aging, Alzheimer's and Parkinson's disease), and activate brain cell neurons against peroxide mediated injury.[**156**] CeO_2 NPs inhibited ROS-induced damage of the neuronal cell line (HT22) in vitro,[**157**] and can protect normal cells during radiation therapy of tumor cells due to inter/intra pH differences in both cell types, and promote the activity of Amifostine against radiation-induced damage.[**158, 159**]

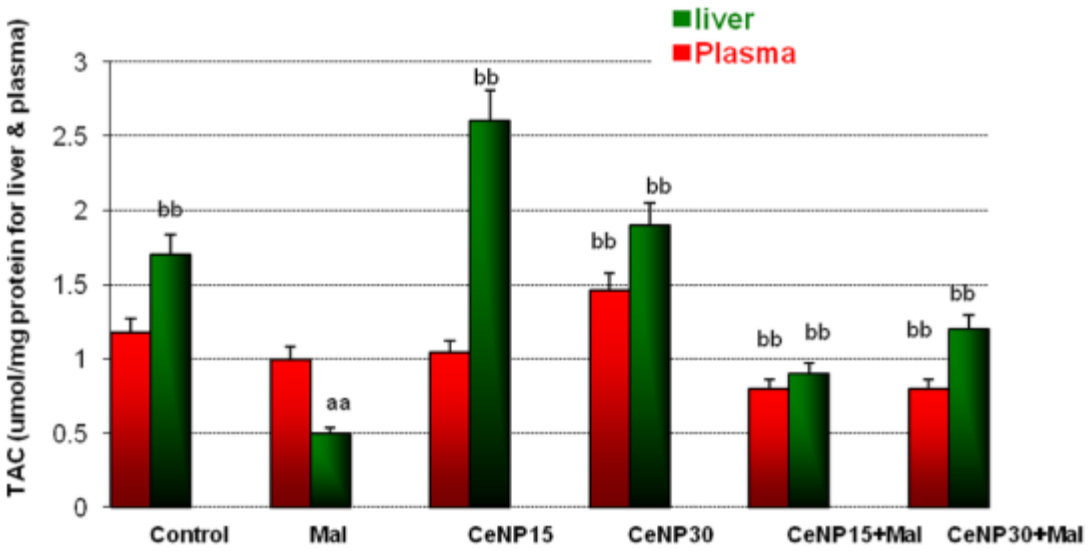

Figure 4. Serum Total Antioxidant Activity profile of cerium nanoparticle in liver homogenate and serum of rat. CeNP: Cerium Nanoparticle, CeNP+ Mal: Cerium Nanoparticle + Malathion.[**160**]

In liver homogenate and serum of rat the total antioxidant activity is enhanced by introduction of cerium nanoparticles and their conjugation with malathion.[**160**] Interestingly, addition to Zn doped CuO ($Cu_{0.89}Zn_{0.11}O$) NPs effectively showed POD mimetic activity against different substrates (including TMB (3,3',5,5'-tetramethylbenzidine), OPD (o-phenylenediamine), ABTS (2,2'-azino-bis(3 ethylbenzothiazoline-6-sulphonic acid)) in the presence of H_2O_2via Michaelis−Menten enzymatic pathways (validated by EPR and fluorescence spectroscopy). Using the peroxidase mimetic activity of $Cu_{0.89}Zn_{0.11}O$ enabled the successful detection of very low amounts of glucose (0.27 ppm) and three antioxidants (specifically tannic acid, ascorbic acid and tartaric acid) by quenching H_2O_2 mediated oxidation of TMB.[**161**]

Among the class of metal oxide NPs, CeO_2 is a ROS scavenger rather than a ROS generator (in comparison to CuO), as evident from Kitchin *et. al.*[**162**] The juxtaposed attitude of CeO_2 such as pro-oxidant and anti-oxidant material is overruled due to plenty of applications of CeO_2 as ROS scavenger e.g., catalase mimetic [**163**], SOD mimetic[**164**] oxidase[**165**] and peroxidase mimetic activities[**166**], Diabetes[**167**] pancreatic beta cell preservation[**168**] Protection from radiation induced-injury[**169**] Liver protective activities[**170**] etc. Caputo *et. al.* reported CeO_2 NPs protected the HaCaT cells from UVB-induced damage, in contrast with TiO_2 with identical shape and size.[**171**]. CeO_2 NPs did not exhibit any toxicity to Jurkat cells that were exposed to UVA, UVB or UVC stimulation and prevented UV-induced mutagenesis and DNA damage [**172**] In case of oxidative stress-induced human cell lines, CeO_2 NPs proved itself as an excellent ROS scavenger where PEGylated CeO_2 NPs protects human keratinocytes (HaCaT cells) from oxidative insult caused by BSO (Buthionine sulfoximine). BSO inhibits the γ-glutamylcysteinesynthetase (γ-GCS) enzyme and thus depletes glutathione (GSH) which is used to modulate the cellular redox potential. GSH acts as natural ROS scavenger in $_2$mammalian cell whose depletion encourages ROS production. The CeO_2 NPs effectively inhibited intracellular ROS production from BSO incubated human keratinocytes (HaCaT) cells.[**52**] Another report suggested that nano CeO_2 (size of 25 nm) replenished GSH level in human breast (MCF-7) and fibrosarcoma (HT-1080) cells assaulted

by ZnO NPs induced oxidative stress. Their investigation revealed that the intracellular ROS of both cell types was increased by 1.65 times higher in MCF-7 and 1.43 times in HT-1080 cells in presence of ZnO NPs but no significant ROS elevation was observed in presence of CeO_2 confirming nontoxicity of CeO_2. Surprisingly incorporation of CeO_2 (100μg/mL) promoted the GSH level in both cell types by 1.56 times in MCF-7 cells and 1.4 times in HT-1080 cells in presence of ZnO NPs.[**173**] The protecting ability of CeO_2 NPs against human cell lines insulted by oxidative stress was further evident from the investigation performed by Rubio and his group. In their work human epithelial lung cell line, BEAS-2B was incubated with $KBrO_3$ that acts as oxidative stress-inducing agent. The intracellular ROS level was reduced for the treated cell with $KBrO_3$ in presence of CeO_2 and similar reduction was also observed in DNA Damage. There was also down regulation of the expression of the Ho1 and Sod2 genes in pretreated cells with CeO_2.[**174**] Hybrid metal oxide nanostructures also exhibit antioxidant behavior which can be used in cancer therapy, for example, Fe_3O_4@C NPs surface modified with folic acid. Studies of the POD mimetic activity of the NPs in the presence of H_2O_2 showed the folic acid shell of the Fe_3O_4@C NPs facilitates electron transfer in the catalytic decomposition of H_2O_2which increased the production of $^{\cdot}OH$, consequently, the Fe_3O_4@C/FA NPs promoted ascorbic-induced oxidative stress in human prostate cancer PC-3 cells in vitro via accumulating ROS with little damage to normal HEK 293T cells.[**148**]

Although fullerene is proven as potential candidate for PDT of cancer cell treatment [**175**] but it can also be protective against oxidative cell damage. Carboxyfullerene (the carboxylic acid derivative of fullerene) is a potential scavenger of $^{\cdot}OH$ and $O_2^{\cdot-}$, [**176**] and such NPs can reduce cytotoxic cell death induced by N-methyl D-aspartate treatment of cortical neurons and delay the onset of death of wild type and mutant SOD (G93A) animals due to amyotrophic lateral sclerosis. Fullerene NPs also prevented the lipid peroxidation induced by $^{\cdot}OH$ and $O_2^{\cdot}$[**177**] and prevented lung injury in an in vivo ischemia model.[**178**] Pristine fullerene protected rats against carbon tetrachloride-induced injury.[**179**]Subcellular localization of fullerenes in the mitochondria of treated cells compensated lack of protein catalyst in mitochondrial SOD knockout mice as well as delayed onset of premature death with a three-fold increase in total lifespan.[**180**] Thus fullerene can compete with degenerative effects of ROS in living cells. This benign feature of fullerenes may be helpful for drug delivery in skin therapy, HIV infection etc.[**181**]

Crossover between Antioxidant and Pro-Oxidant Activity-Duality of Metal oxide Nanostructure and Their Composites.

Crossover between antioxidant and pro-oxidant activity is a very rare phenomenon in materials with the exception in ascorbic acid (Vitamin C) which exhibits antioxidant activity at higher concentrations and pro-oxidant activity at lower concentrations depending upon the ratio of ascorbic acid and catalytic metal ions such as copper and iron present in food products.[**182**] Crossover phenomena are observed in antioxidants found in dietary supplements (e.g., ascorbic acid, L-cysteine, L-glutathione, and (−)-epigallocatechin gallate) in the presence of copper (at pH 1.2 and 7.4 when the molar ratio of antioxidants (1 mM) to Cu^{2+} (0.1mM) was 10, quantified by EPR spectra by the application of DMPO (a spin trap agent for $^{\cdot}OH$) and H_2O_2).[**183**] The generation of ROS ($^{\cdot}OH$) after mixing Cu^{2+} and the antioxidant (Ascorbate, $AscH^-$) is described below: [**183**]

$$Cu^{2+}AscH \rightarrow Cu^{+} + Asc^{-} + H^{+} \quad (13)$$

$$Cu^{+} + H_2O_2 \rightarrow Cu^{2+} + \cdot OH + OH^{-} \quad (14)$$

The EPR intensity of the spin adduct DMPO-OH was lower at pH 7.4 as compared to pH 1.2 due to the relatively poor solubility of Cu^{2+} at pH 7.4 and the order of pro-oxidant activity at both pH is: L-cysteine >ascorbic acid > EGCG > GSH.

Similarly, antioxidant activity was observed for molar ratio of antioxidants (10 mM) to Cu^{2+} (0.1mM). Ascorbic acid, GSH and EGCG only exhibited lowered EPR intensity of DMPO-OH adduct both at pH 1.2 and 7.4. [**180**] Yin *et al*. had proposed two mechanisms for such activity (including reduction of ·OH formation by limiting Cu^{2+} redox cycle observed for GSH only and interception of ·OH formation before targeting DMPO to form DMPO-OH which is only applicable for ascorbic acid and EGCG).[**183**] Interestingly L-cysteine did not show any antioxidant activity due to rapid formation of ·OH, which was extended to ·OH generation in bovine serum albumin by GSH and L-cysteine. [**183**]

Crossover can happen in the absence of catalytic metal ions as successfully demonstrated by Lu *et. al*. using nano CeO_2,[**184**] wherein different concentrations of ·OH, different morphology and size of CeO_2nanomaterials demonstrate crossover phenomena. UV-Vis spectroscopy using methyl violet (MV) was employed for quantitative elucidation of this crossover phenomenon; two different morphologies e.g., spherical ceria NPs with sizes of ~5-20 nm, and nanocubes with sizes of 20-40 nm were employed, yielding amounts of Ce^{3+} ionic species present in NPs and nanocubes in the range of ~31-28% and 26-25%, respectively, which control antioxidant activity (·OH scavenging) of CeO_2. Different concentrations of ·OH were employed, with $nCeO_2$ showing antioxidant activity at low dosages of ·OH and pro-oxidant activity at high levels of ·OH content. Additionally with increasing concentrations of $nCeO_2$, it exhibited protective effect against ·OH, and then showed oxidant activity at higher concentrations, resulting in the conclusion that $nCeO_2$ exhibits antioxidant activity at low ·OH and ceria concentrations, and show oxidant activity at high concentrations of ·OH and ceria, and that larger Ce^{3+} contents could act as a ·OH source as well as catalyst of Fenton like reactions.[**184**]

$$Ce^{3+} + H_2O_2 \rightarrow Ce^{4+} + \cdot OH + OH^- \quad (15)$$

Ce^{3+} can act as an antioxidant, but concentrations of Ce^{3+}that are high lead to pro-oxidant activity. Size factors also play an important role in such crossover with smaller NPs irrespective of concentrations exhibiting pro-oxidant activity due to presence of larger concentrations of Ce^{3+} ions at their surfaces. Morphology strongly affects antioxidant and pro-oxidant behavior of nano ceria, at the same concentration (50 μ M) NPs act as oxidants, whereas nanocubes act as antioxidants, which may be due to Ce^{3+} content. [**184**]

Similar crossover phenomenon was observed for graphene quantum dots (GQDs) but the controlling factor is the presence of light.[**185**] GQDs (sizes of ~3-6 nm) scavenges ·OH, $O_2^{\cdot-}$ and 1,1-Diphenyl-2-picrylhydrazyl (DPPH) radicals in a concentration-dependent manner (quantified by EPR spectra) in the dark. Such activity was highlighted in protection of HUVEC cells against oxidative damage caused by H_2O_2 treatment and X-ray irradiation. GQD exposure of 405 nm light increased intracellular ROS generation and reduced cell viability (and the generation of $^1O_2$, ·OH and $O_2^{\cdot-}$shown by EPR measurements after 405 nm light irradiation). GQDs generated $^1O_2$ by both energy transfer and electron transfer pathways and ·OH as well as $O_2^{\cdot-}$ were generated from electron-hole pair generation and charge separation. These in vitro ROS may involve elevated levels of intracellular ROS generation in A549 cells and promotion of oxidation of non-enzymatic antioxidants ascorbic acid and GSH, as well as causing lipid peroxidation leading to cell death.[**185**]

MgO nanostructures also display crossover between pro-oxidant and antioxidant activities, wherein concentration- and morphology-dependent crossover phenomena occur due to overdamping of F^{2+} defect states responsible for $O_2^{\bullet-}$ scavenging and the development of F_2^{3+}, F_2^{+} , and F^{+} states that are responsible for $O_2^{\bullet-}$generation. F^{2+} defect states behave as acceptor levels and F_2^{3+}, F_2^{+} , and F^{+} function as donor levels, the lower the concentration the deeper the F^{2+} defect states and at higher concentrations F_2^{3+}, F_2^{+} , and F^{+} states are developed due to suppression of F^{2+},and successful crossover occurs at 200 μg/mL. The prooxidant activity was estimated by measuring antibacterial activity and interactions with the antioxidant defense system like ascorbic acid proved the crossover phenomenon; successful crossover also predicts the possibility of MgO nanostructures as potential cancer therapeutic agent with low adverse effects on normal cells.[**29**]

ROS-Induced Anticancer Activity of Metal oxides Nanostructures and Their Composites

ROS at higher levels oxidizes macromolecules and causes mitochondrial dysfunction in living cells due to release of oxidative stress which eventually causes cell apoptosis.[**186**] Ideally a ROS generating antibacterial agent should have low cytotoxicity at appropriate concentrations.[**187**] Studies do not always yield clear results, for example studies of cytotoxicity of GO@CS/ZnO against peripheral blood mononuclear cells (PBMC) over a wide concentration range (1-250 μ g/ml) where low cytotoxicity (up to 80% viability) was observed up to 25 μ g/ml, however, investigation of ROS mediated antibacterial activity at 2.5-5 μ g/ml found significant intracellular ROS.[**143**]

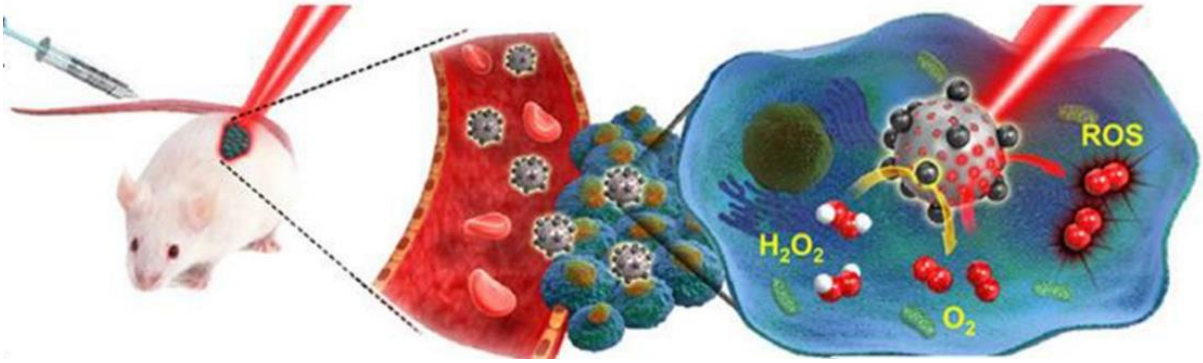

Figure 5. Photodynamic Therapy of $MnFe_2O_4$ conjugated mesoporous silica nanoparticle via singlet oxygen ($O_2^{\cdot-}$) generation**.[189]**

ROS-induced anticancer therapy utilizing metal oxides with UV light irradiation as a means of photodynamic therapy.[**188**] Such light-induced ROS can damage DNA, cell membrane and proteins leading to cell death.[**7**] In this therapeutic approach, singlet oxygen($O_2^{\cdot-}$) generation and its exposure onto targeted cell is encouraged. Mesoporous silica nanoparticle exhibited such activity in hypoxia tumor.[**189**] Toxicity in lysosomes was observed after exposure of ZnO due to release of ROS and Zn^{2+} ions.[**76,190**] Another report suggests light-induced ROS of ZnO NPs as prime factor for apoptosis of cancer cells (HL60), glioma cells and rat retinal ganglion cells.[**191,192**] ROS-induced toxicity of Fluorescein isothiocyanate/ZnO (FITC/ZnO) composites in cervical cancer (HeLa) and breast cancer (MCF-7) cells with low cytotoxicity towards fibroblast cells (L929), as demonstrated via studies of cell apoptosis, DNA fragmentation, depolarization of mitochondrial membranes and cell cycle arrest at the S phase.[188] Several reports produced evidence of cancer cell

killing via intracellular ROS pathways by ZnO NPs.[**193-195**] MgO NPs can potentially be employed in cancer therapy, as demonstrated with HeLa, SNU-16 and AGS cells along with normal human lung fibroblast cells CCD-25Lu,were all cancer cells were affected by MgO NPs, yet normal cells were unaffected.[**196**] $DCFH_2$-DA was used to probe intracellular ROS generated in cancer cells, finding that the cancer cell inhibition by MgO NPs is entirely mediated by ROS generation due to the presence of oxygen vacancies at the surface of NPs.[**196**]

Hybrid metal oxide nanostructures had been utilized in cancer therapy,[**159**] core shell structures of $Fe_3O_4$with carbon (C) shells promote cancer cell inhibition by ascorbic acid which has low in vivo efficacy at tolerable dosages.[**148**] Ideally ascorbic acid alters the normal redox state of cell thereby promoting ROS generation that kills cancer cells. In order to bind the receptor specifically, Fe_3O_4@C NPs were modified by folic acid on the surface and subsequently peroxidase (POD) mimetic activity was conducted in the presence of H_2O_2. The carbon shell of NPs facilitates electron transfer in the catalytic decomposition of H_2O_2 (POD activity) which promotes the production of $^{\cdot}OH$ which promotes ascorbic acid-induced oxidative stress in cultured human prostate cancer PC-3 cells via accumulating ROS. Additionally, the NPs caused little damage to normal cells (HEK 293T cells).[**148**]There are opportunities for further elucidation of the mechanism of anticancer activity mediated by specific ROS (e.g., from metal oxides) that are specifically cancer cell killing whilst demonstrating low cytotoxicity towards normal cells. ROS-induced anticancer activity is also evident from Ag_3PO_4/Polyindole nanocomposite as reported by Podder *et. al.*[**144**] where Ag_3PO_4:Polyindole= 2:1 and 1:1 exhibited enhanced anticancer activity against MCF-7 breast cancer cell with concomitant elevated intracellular ROS level. ZnO NPs exhibited anticancer activity via oxidative stress pathways as evident from recent reports [**197,198**] but its composites with SnO_2 and graphene oxide e.g., SnO_2-ZnO and SnO_2-ZnO/rGO nanocrystals render the enhancement in anticancer activity. They fundamentally upregulated the mRNA expression level of the Caspase-3 gene in a dose-dependent manner (10–50 μg/mL) and also increased the intracellular ROS generation with simultaneous GSH depletion in a dose dependent manner. SnO_2-ZnO/rGO nanocrystals exhibited superior activity towards these experimentations.[**199**] Ag-TiO_2 hybrid nanorod killed 4T1 breast cancer cell line by inducing $^1O_2$ under UV irradiation with intensity 5.6 $mW{\cdot}cm^{-2}$. This photodynamic therapy essentially involved accumulation of the nanohybrid in the 4T1 cancer cell and exertion of ROS under UV light stimulation.[**200**] Nagajyothi *et. al.* had reported ROS mediated anticancer activity of ZnO-Ag nanocomposite against HeLa and SKOV-3 cell. ZnO nanoflakes with 0.75mmol Ag exhibited remarkable anticancer activity towards the two types of cell where the cell viability was drastically reduced in presence of the nanocomposite. The anticancer activity essentially based on apoptosis of the cells where the ATP production inside the cells were largely inhibited in presence of the nanocomposite implying disruption of mitochondrial respiratory chain and DNA damage. The mechanism behind this disruption is the elevation in intracellular ROS-induced by the nanocomposite. The synergistic effect on anticancer activity was developed from the betacyanins, beetroot components which are potent anticancer agents. [**201**]

Conclusion and Outlook

This review highlights the implementation of toxicity as well as gentleness of different nanomaterials including metallic, non-metallic, metal oxide NPs and their nanocomposites. The toxicity is attributed to generation of different free radicals $O_2^{\cdot-}$, $^{\cdot}OH$, H_2O_2 and $^1O_2$. The interrelation of ROS generation and the electronic structure of the nanomaterials as well as

surface modifications are explored that will be helpful to design nanomaterials with predictable behaviors. ROS-induced antibacterial activity of nanomaterials and its correlation with time responses (even in dark conditions) open up potential opportunities of such materials for antimicrobial applications. Furthermore, the ROS scavenging and translational phenomena of anti-oxidant property to pro-oxidant behavior offers scope to design nanomaterials as novel cancer therapeutic agents with minimal adverse side effects to normal healthy cells. Future research and development will focus on fundamental understanding of such materials and their biological activities, and the applied studies will be helpful to clinical up gradation for better living.

Conflict of Interest

The authors declare no conflicts of interest.

Acknowledgements

We acknowledge the Department of Science & Technology of the Government of India, for financial assistance for S.P. through the DST-INSPIRE program (Grant No. DST/INSPIRE Fellowship/2014/82). J.G.H. acknowledges support from a Royal Society Research Grant (Grant No. RG160449).

Conflict of Interest

The authors declare no conflicts of interest.

References

1. J. Gupta, K.C. Barick, D. Bahadur. Defect mediated photocatalytic activity in shape-controlled ZnO nanostructures. Journal of Alloys and Compounds. **509**, 6725–6730 (2011).
2. H. Chibli, L. Carlini, S. Park. Dimitrijevic, N. M., Nadeau, J. L.Cytotoxicity of InP/ZnS quantum dots related to reactive oxygen species generation, Nanoscale. **3**, 2552 (2011)
3. Li. Yang, N. Junfeng, Z. Wen, Z. Lilan, S. Enxiang. Influence of Aqueous Media on the ROS-Mediated Toxicity of ZnO Nanoparticles toward Green Fluorescent Protein-Expressing Escherichia coli under UV-365 Irradiation, Langmuir.**30**, 2852−2862 (2014).
4. S. Podder, S. Halder, A. Roychowdhury, D. Das, C. K. Ghosh, Superb hydroxyl radical-mediated biocidal effect induced antibacterial activity of tuned ZnO/chitosan type II heterostructure under dark. J. Nanopart. Res. **18**, 294 (2016)
5. V. L. Prasanna, R. Vijayaraghavan. Insight into the Mechanism of Antibacterial Activity of ZnO: Surface: Defects Mediated Reactive Oxygen Species Even in the Dark. Langmuir. **31**, 9155−9162 (2015).
6. J. Y. Chen, Y. M. Lee, D.,N. Zhao, K. Mak, R. N. Wong, W. H. Chan, N. H. Cheung, Quantum dot-mediated photoproduction of reactive oxygen species for cancer cell annihilation. Photochem. Photobiol., **86**, 431–437 (2010).
7. W. Zhang, Y. Li, J. Niu, Y. Chen, Photogeneration of reactive oxygen species on uncoated silver, gold, nickel, and silicon nanoparticles and their antibacterial effects, Langmuir, **29**,4647–465 (2013).
8. J. S. Blanksby, V. M. Bierbaum, G. B. Ellison, S. Kato. Superoxide Does React with Peroxides: Direct Observation of the Haber–Weiss Reaction in the Gas Phase, Angew. Chem. Int. Ed.,**46**, 4948–4950 (2007).

9. V. M. Kiseleva, I. M. Kislyakov, A. N. Burchinova, Generation of Singlet Oxygen on the Surface of Metal Oxides, Optics and Spectroscopy. **120**, 520–528 (2016).
10. L. Yang, W. Zhang., J, Niu., Y. Chen. Mechanism of Photogenerated Reactive Oxygen Species and Correlation with the Antibacterial Properties of Engineered Metal-Oxide Nanoparticles. ACS Nano. **6**, 5164-5173 (2012).
11. Y. Liua, S. Zhua, Z. Gua, C. Chena, Y. Zhao, Toxicity of manufactured nanomaterials, Particuology. **69,** 31–48 (2022).
12. H. Bouwmeester, I. Lynch, H. J. P. Marvin, K. A. Dawson, M. Berges, D. Braguer. Minimal analytical characterization of engineered nanomaterials needed for hazard assessment in biological matrices. Nanotoxicology. **5**, 1–11 (2011).
13. A. Samanta, S. Podder, C. K. Ghosh, M. Bhattacharya, J. Ghosh, A. K. Mallik, A. Dey, A. K. Mukhopadhyay, ROS mediated high anti-bacterial efficacy of strain tolerant layered phase pure nano calcium hydroxide, Journal of the Mechanical Behaviour of Biomedical Materials, **72**, 110–128 (2017).
14. N. Biswas, A. Samanta, S. Podder, C. K. Ghosh, J. Ghosh, M. Das, A. Mallik, A. Mukhopadhyay, Phase Pure, High Hardness, Biocompatible Calcium Silicates with Excellent Anti-bacterial and Biofilm Inhibition Efficacies for Endodontic Applications, Journal of the Mechanical Behaviour of Biomedical Materials. **86**,264-283 (2018).
15. A. Samanta, S. Podder, M. Kumarasamy, C. K. Ghosh, D. Lahiri, P. Roy, S. Bhattacharjee, J. Ghosh, A. K. Mukhopadhyay, Au Nanoparticle-Decorated Aragonite Microdumbells for Enhanced Antibacterial and Anticancer Activities, Materials Science and Engineering: C. **103**,109734 (2019).
16. X. Ma, Y. Wang, X.-L. Liu, H. Ma , G. Li , Y. Li , F. Gao, M. Peng, , H. M. Fan , X. J. Liang, Fe_3O_4–Pd Janus nanoparticles with amplified dual-mode hyperthermia and enhanced ROS generation for breast cancer treatment. Nanoscale Horiz., **4**, 1450-1459 (2019)
17. A. Poma, G. Vecchiotti, S. Colafarina, O. Zarivi, M. Aloisi, L. Arrizza, G. Chichiriccò, P. D. Carlo, In Vitro Genotoxicity of Polystyrene Nanoparticles on the Human Fibroblast Hs27 Cell Line. Nanomaterials.**9**, 1299 (2019).
18. Z. Hu, Y. Ding. Cerium oxide nanoparticles-mediated cascade catalytic chemo-photo tumor combination therapy. Nano Res. **15,** 333–345 (2022)]
19. J. Chen, T. Fan, Z. Xie, Q. Zeng, P. Xue, T. Zheng, Y. Chen, X. Luo, H. Zhang, Advances in Nanomaterials for Photodynamic Therapy Applications: Status and Challenges, Biomaterials, **237**, 119827 (2020).
20. Y. Hou, A. Mushtaq, Z. Tang, E. Dempsey, Y. Wu, Y. Lu, C. Tian, J. Farheen, X. Kong, M. Z. Iqbal, Journal of Science: Advanced Materials and Devices. (2021) https://doi.org/10.1016/j.jsamd.2022.100417.
21. Y. Yamakoshi, N. Umezawa, A. Ryu, K. Arakane, N. Miyata, Y. Goda, T. Masumizu, T. Nagano. Active Oxygen Species Generated from Photoexcited Fullerene (C_{60}) as Potential Medicines: $O_2^{\cdot -}$ versus $^1O_2$. J. Am. Chem. Soc. **125**, 12803-12809 (2003)
22. L. Valgimigli, A. Baschieri, R. Amorati. Antioxidant activity of nanomaterials, Journal of Materials Chemistry B, **6**, 2036 (2018)
23. A. Chakraborty, N. R. Jana, Vitamin C-Conjugated Nanoparticle Protects Cells from Oxidative Stress at Low Concentrations but Induces Oxidative Stress and Cell Death at High Concentrations. ACS Appl. Mater. Interfaces. **9**, 41807−41817 (2017)
24. H. Palafox-Carlos, J. H. Ayala-Zavala, C. A.́ Gonzalez-Aguilar. The Role of Dietary Fiber in the Bioaccessibility and Bioavailability of Fruit and Vegetable Antioxidants. J. Food Sci. **76**, R6−R15 (2011).
25. L. Rubio, B. Annangi, L. Vila, A. Hernández, R. Marcos. Arch Toxicol, (2015). https://doi.org/10.1007/s00204-015-1468-y.

26. L. Fan, P. Sun, Y. Huang, Z. Xu, X. Lu, J. Xi, J. Han, R. Guo, ACS Appl. Bio Mater. (2020) https://doi.org/ 10.1021/acsabm.9b01079.
27. M. Pooyan, G. Matineh, P. Vinod, V.T., S. Faezeh, A. Milad, A. Sina, P. Nahid, Z. Ali, N. Zare, E. Kooti, M. Mokhtari, B. Borzacchiello, A. Tay, R. Franklin, ACS Applied Nano Materials. (2020) https://doi.org/ 10.1021/acsanm.0c01164.
28. Y. Zheng, X. Hong, J. Wang, L. Feng, T. Fan, R. Guo, H. Zhang, 2D Nanomaterials for Tissue Engineering and Regenerative Nanomedicines: Recent Advances and Future Challenges, Adv. Healthcare Mater. **10**, 2001743 (2021)
29. S. Podder, D. Chanda, A,K. Mukhopadhyay, A. De, B. Das, A. Samanta, J.G. Hardy, C. K. Ghosh, The impact of morphology and concentration on crossover between antioxidant and pro-oxidant activity of MgO nanostructures. Inorg. Chem. **57**, 12727-12739 (2018).
30. Z.-M. Xiu, J. Ma, P. J. J. Alvarez, Differential Effect of Common Ligands and Molecular Oxygen on Antimicrobial Activity of Silver Nanoparticles versus Silver Ions, Environ. Sci. Technol.**45**(20), 9003–9008 ((2011)
31. J. R. Nakkala, R. Mata, K. Raja, V. K. Chandra, S. R. Sadras, Green synthesized silver nanoparticles: Catalytic dye degradation, **in vitro** anticancer activity and **in vivo** toxicity in rats, Materials Science and Engineering: C, **91**(1) 372-381(2018).
32. V. Karthika, A. Arumugam, K. Gopinath, P. Kaleeswarran, M. Govindarajan, N.S. Alharbi, S. Kadaikunnan, J. M. Khaled, G. Benelli, **G.** ulmifolia. bark-synthesized Ag, Au and Ag/Au alloy nanoparticles: Photocatalytic potential, DNA/protein interactions, anticancer activity and toxicity against 14 species of microbial pathogens, Journal of Photochemistry and Photobiology B: Biology, **167**, 189-199 (2017).
33. L. P. Datta, A. Chatterjee, K. Acharya, P. De, M. Das, Enzyme responsive nucleotide functionalized silver nanoparticles with effective antimicrobial and anticancer activity, New J. Chem., **41**, 1538-1548(2017).
34. M. J. Llansola, P. M. David Gara, M. L. Kotler, S. Bertolotti, E. San Roman, H. B. Rodriguez, M. C. Gonzalez, Silicon Nanoparticle Photophysics and Singlet Oxygen Generation. Langmuir, **26**, 10953-10960 (2010).
35. M. Fujii, M. Usui, S. Hayashi, E. Gross, D. Kovalev, N. Kunzner, J. Diener, V. Y. Timoshenko, Chemical Reaction Mediated by Excited States of Si Nanocrystals - Singlet Oxygen Formation in Solution. J. Appl. Phys.**95**, 3689-3693 (2004).
36. D. Kovalev, E. Gross, N. Kunzner, F. Koch, V. Y. Timoshenko, M. Fujii, Resonant Electronic Energy Transfer from Excitons Confined in Silicon Nanocrystals to Oxygen Molecules. Phys. Rev. Lett. **89**,137401 (2002).
37. S. Bhattacharjee, L. H. J. de Haan, N. M. Evers, X. Jiang, A. Marcelis, H. Zuilhof, I. M. C. M. Rietjens, G. M. Alink, Role of Surface Charge and Oxidative Stress in Cytotoxicity of Organic Monolayer-Coated Silicon Nanoparticles towards Macrophage NR 8383 Cells. Par. FibreToxicol.**7**, 25 (2010).
38. L, Ruizendaal, S. Bhattacharjee, K. Pournazari, M. Rosso-Vasic, L.H. J. de Haan, G. M. Alink Marcelis, Z. H. ATM, Synthesis and cytotoxicity of silicon nanoparticles with covalently attached organic monolayers. Nanotoxicology **3**(4), 339-347 (2009).
39. S. T. Kim, K. Saha, C. Kim, V. M. Rotello, The Role of Surface Functionality in Determining Nanoparticle Cytotoxicity, ACCOUNTS OF CHEMICAL RESEARCH, **46**(3) 681–691 (2013)
40. N. M Schaeublin ,L.K. Braydich-Stolle, A. M Schrand, J. M Miller, J. Hutchison, J. J Schlager, S. M Hussain, Surface charge of gold nanoparticles mediates mechanism of toxicity, **3**, 410-420 (2011).
41. C. M Goodman , C. D McCusker, T. Yilmaz, V. M Rotello, Toxicity of gold nanoparticles functionalized with cationic and anionic side chains, Bioconjugate Chem. 15, 4, 897–900(2004).

42. S. Hussain, K. Hess, J. Gearhart, K. Geiss, J. Schlager, In Vitro Toxicity of Nanoparticles in BRL 3A Rat Liver Cells. Toxicol. Vitro **19**, 975-983 (2005).
43. R. Foldbjerg, P. Olesen, M. Hougaard, D. A. Dang, H. J. Hoffmann, H. Autrup, PVP-coated silver nanoparticles and silver ions induce reactive oxygen species, apoptosis and necrosis in THP-1 monocytes. Toxicol. Lett. **190**, 156-162 (2009)
44. C. Carlson, S. M. Hussain, A. M. Schrand, L. K. Braydich-Stolle, K. L. Hess, R. L. Jones, J. J. Schlager, Unique cellular interaction of silver nanoparticles: size-dependent generation of reactive oxygen species. J. Phys. Chem. B **112**, 13608-13619 (2008).
45. O. Choi, Z. Hu, Size Dependent and Reactive Oxygen Species Related Nanosilver Toxicity to Nitrifying Bacteria, Environ. Sci. Technol. 42, 4583–4588 (2008).
46. Li, X.; Lenhart, J. J.; Walker, H. W. Aggregation kinetics and dissolution of coated silver nanoparticles. Langmuir 2012, 28 (2), 1095-1104,
47. J. Fabrega, S. R. Fawcett, J. C. Renshaw, J. R. Lead, Silver nanoparticle impact on bacterial growth: effect of pH, concentration, and organic matter. Environ. Sci. Technol. **43** (19), 7285-7290 (2009).
48. Y. Li, W. Zhang, J. Niu, Y. Chen, Surface coating–dependent dissolution, aggregation, and ROS generation of silver nanoparticles under different irradiation conditions, Environ. Sci. Technol. **47**, 18, 10293–10301(2013).
49. J. Liu, R. H. Hurt, Ions release kinetics and particle persistence in aqueous nano-silver colloids. Environ. Sci. Technol. **44** (6), 2169-75 (2010).
50. V. Bastos , J.M.P. Ferreira de Oliveira , D. Brown , H. Jonhston , E. Malheiro , A.L. Daniel-da-Silva , I.F. Duarte , C. Santos, H. Oliveira, The influence of Citrate or PEG coating on silver nanoparticle toxicity to a human keratinocyte cell line, Toxicology Letters **249** 29–41 (2016).
51. Y. Pan, A. Leifert, D. Ruau, S. Neuss, J. Bornemann, G. Schmid, W. Brandau, U. Simon, , W. Jahnen-Dechent, Gold Nanoparticles of Diameter 1.4 nm Trigger Necrosis by Oxidative Stress and Mitochondrial Damage. Small.**5**, 2067-2076, (2009).
52. R. Singh, A. Singh Karakoti, W. T Self, S. Seal, S. Singh, Langmuir.(2016) **https://doi.org/10.1021/acs.langmuir.6b03022**.
53. M. Misawa, J. Takahashi, Generation of Reactive Oxygen Species Induced by Gold Nanoparticles under X-ray and UV Irradiations. Nanomed.- Nanotechnol. Biol. Med. **7**, 604-614, (2011)
54. R. Ramachandran, C. Krishnaraj, V. K. Abhay Kumar, S. L. Harper, T. P. Kalaichelvan, S.-Il. Yun, In vivo toxicity evaluation of biologically synthesized silver nanoparticles and gold nanoparticles on adult zebrafish: a comparative study, Biotech, **8**,441 (2018).
55. S. Sabella, V. Brunetti, G. Vecchio, A. Galeone, G. Maiorano, R. Cingolani, P. Paolo Pompa, J Nanopart Res, **13**,6821–6835 (2011).
56. J. Farkas, P. Christian, J. A. G. Urrea, N. Roos, M. Hassellov, K. E. Tollefsen, K. V. Thomas, Effects of Silver and Gold Nanoparticles on Rainbow Trout (Oncorhynchus Mykiss) Hepatocytes. Aquat. Toxicol. **96**, 44-52, (2010)
57. D. Raghunandan, B. Ravishankar, G. Sharanbasava, D. Mahesh, V. Harsoor, M. Yalagatti, M. Bhagawanraju, A. Venkataraman, Anti-Cancer Studies of Noble Metal Nanoparticles Synthesized Using Different Plant Extracts. Cancer Nanotechnol. **2**, 57-65, (2011)
58. Y. Cui, Y. Zhao, Y. Tian, W. Zhang, X. Lu, X. Jiang. The Molecular Mechanism of Action of Bactericidal Gold Nanoparticles on Escherichia coli. Biomaterials **33**, 2327-2333, (2012).

59. C. A. J. Dick, D. M. Brown, K. Donaldson, V. Stone. The Role of Free Radicals in the Toxic and Inflammatory Effects of Four Different Ultrafine Particle Types. Inhal. Toxicol. **15**, 39-52 (2003).
60. M.M. Mohamed, S.A. Fouad, H.A. Elshoky, G.M .Mohammed, T.A. Salaheldin, Antibacterial effect of gold nanoparticles against Corynebacterium pseudotuberculosis. Int. J. Vet. Sci. Med. **5**, 23–29 (2017).
61. M. Shi, H. S. Kwon, Z. Peng, A. Elder, H. Yang, Effects of Surface Chemistry on the Generation of Reactive Oxygen Species by Copper Nanoparticles, **6**(3), 2157–2164 (2012).
62. A. Ahmad, Y. Wei, F. Syed, K. Tahir, A. U. Rehman, A. Khan, S. Ullah, Q. Yuan, The effects of bacteria-nanoparticles interface on the antibacterial activity of green synthesized silver nanoparticles, Microbial Pathogenesis, **102**, 133-142 (2017).
63. K. Peters, R. E. Unger, A. M. Gatti, E. Sabbioni, R. Tsaryk, C. J. Kirkpatrick, Metallic Nanoparticles Exhibit Paradoxical Effects on Oxidative Stress and Pro-Inflammatory Response in Endothelial Cells in Vitro. Int. J. Immunopathol. Pharmacol. **20**, 685-695, (2007).
64. T. Xia, M. Kovochich, J. Brant, M. Hotze, J. Sempf, T. Oberley, C. Sioutas, J. I. Yeh, M. R. Wiesner, A. E. Nel, Comparison of the Abilities of Ambient and Manufactured Nanoparticles to Induce Cellular Toxicity According to an Oxidative Stress Paradigm. Nano Lett. **6**, 1794-1807 (2006).
65. S.-H. Hwang, F. Thielbeer, J. Jeong, Y. Han, S.V. Chankeshwara, M. Bradley, W.-S. Cho, Dual contribution of surface charge and proteinbinding affinity to the cytotoxicity of polystyrene nanoparticles in nonphagocytic A549 cells and phagocytic THP-1 cells, JOURNAL OF TOXICOLOGY AND ENVIRONMENTAL HEALTH, PART A, **79**, 925-937 (2016)
66. Z. Markovic, B. Todorovic-Markovic, D. Kleut, N. Nikolic, S. Vranjes-Djuric, M. Misirkic, L. Vucicevic, K. Janjetovic, A. Isakovic, L. Harhaji, The Mechanism of Cell-Damaging Reactive Oxygen Generation by Colloidal Fullerenes. Biomaterials **28**, 5437-5448 (2007).
67. Y. Yamakoshi, N. Umezawa, A. Ryu, K. Arakane, N.Miyata, Y. Goda, T. Masumizu, T. Nagano, Active Oxygen Species Generated from Photoexcited Fullerene (C_{60}) as Potential Medicines: $O_2^{\cdot -}$ versus $^1O_2$. J. Am. Chem. Soc. **125**, 12803-12809 (2003)
68. M. Cho, J. D. Fortner, J. B. Hughes, J. H. Kim, Escherichia Coli Inactivation by Water-Soluble, Ozonated C60 Derivative: Kinetics and Mechanisms. Environ. Sci. Technol. **43**, 7410-7415 (2009)
69. L. Brunet, D. Y. Lyon, E. M. Hotze, P. J. J. Alvarez, M. R. Wiesner, Comparative Photoactivity and Antibacterial Properties of C_{60} Fullerenes and Titanium Dioxide Nanoparticles. Environ. Sci. Technol.**43**, 4355-4360 (2009)
70. J. Lee, J. D. Fortner, J. B. Hughes, J. H. Kim, Photochemical production of reactive oxygen species by C60 in the aqueous phase during UV irradiation. Environ. Sci. Technol. **41**, 2529-2535 (2007).
71. E. M. Dumas, V. Ozenne, R. E. Mielke, J. L. Nadeau, Toxicity of CdTe Quantum Dots in Bacterial Strains. IEEE Trans. Nanobiosci. **8**, 58-64 (2009).
72. M. Green, E. Howman, Semiconductor Quantum Dots and Free Radical Induced DNA Nicking. Chem. Commun. **1**, 121-123 (2005)
73. H. Saito, Y. Nosaka, Mechanism of Singlet Oxygen Generation in Visible-Light-Induced Photocatalysis of Gold-Nanoparticle-Deposited Titanium Dioxide, J. Phys. Chem. C **118**, 15656−15663 (2014)
74. H.Yin, P. S.Casey, M. J. McCall, M. Fenech, Effects of Surface Chemistry on Cytotoxicity, Genotoxicity, and the Generation of Reactive Oxygen Species Induced by ZnO Nanoparticles, Langmuir **26**, 15399–15408 (2010).

75. H. F. Lin, S. C. Liao, S. W. Hung, The DC Thermal Pasma Synthesis of ZnO Nanoparticles for Visible-Light Photocatalyst. J. Photochem. Photobiol. A: Chem. **174**, 82–87 (2005)
76. T. Xia, M. Kovochich, M. Liong, L. Ma dler, B. Gilbert, H. Shi, J. I.. Yeh, J. I.. Zink, A. E. Nel, Comparison of the Mechanism of Toxicity of Zinc Oxide and Cerium Oxide Nanoparticles based on Dissolution and Oxidative Stress Properties. ACS Nano **2**, 2121–213 (2008).
77. D. Schubert, R. Dargusch, J. Raitano, S. W. Chan, Cerium and Yttrium Oxide Nanoparticles are Neuroprotective. Biochem. Biophys. Res. Commun. **342**, 86 (2006).
78. A. Thill, O. Zeyons, O. Spalla, F.Chauvat, J.Rose, M. Auffan, A. M. Flank, Cytotoxicity of CeO_2 Nanoparticles for Escherichia coli. Physico-Chemical Insight of the Cytotoxicity Mechanism. Environ. Sci. Technol. **40**, 6151– 6156 (2006).
79. W. Lin, Y. W. Huang, X. D. Zhou, Y. Ma, Toxicity of Cerium Oxide Nanoparticles in Human Lung Cancer CellsInt. J. Toxicol. **25**, 451–457 (2006).
80. S. Yu , Z. Tong , L. Yi, Z. Jin Cai, Size-dependent hydroxyl radicals generation induced by SiO2 ultra-fine particles: The role of surface iron, Sci China Ser B-Chem , **52**(7),1033-1041 (2009)
81. S. E. Lehman, A. S. Morris, P. S. Mueller, A. K. Salem, V. H. Grassian ,S. C. Larsen, Silica Nanoparticle-Generated ROS as a Predictor of Cellular Toxicity: Mechanistic Insights and Safety by Design, Environ. Sci.: Nano, **3**, 56-66 (2016)
82. L. C. J. Thomassen, A. Aerts, V. Rabolli, D. Lison, L. Gonzalez, M. Kirsch-Volders, D. Napierska, P. H. Hoet, C. E. A. Kirschhock, J. A. Martens, Synthesis and Characterization of Stable Monodisperse Silica Nanoparticle Sols for in Vitro Cytotoxicity Testing, Langmuir **26**(1), 328–335 (2010)
83. Y. JJ, L. J, E. M, R. JE, Fu. PP, M. RP, Z. B Phototoxicity of nano titanium dioxides in hacat keratinocytes-generation of reactive oxygen species and cell damage. Toxicol Appl Pharmacol **263**(1),81–88 (2012).
84. P. Chen, H. Wang , M. He, B. Chen, B. Yang, B. Hu, Size-dependent cytotoxicity study of ZnO nanoparticles in HepG2 cells, Ecotoxicology and Environmental Safety **171**, 337–346 (2019)
85. A. Busra Sengul, E. Asmatulu, Environmental Chemistry Letters, (2020) https://doi.org/10.1007/s10311-020-01033-6
86. E.J Petersen, V. Reipa, S.S Watson, D.L Stanley, S.A Rabb, B.C Nelson DNA damaging potential of photoactivated P25 titanium dioxide nanoparticles. Chem Res Toxicol **27**(10),1877–1884 (2014)
87. A. Lipovsky, Z. Tzitrinovich, H. Friedmann, G. Applerot, A. Gedanken, R. Lubart, EPR Study of Visible Light-Induced ROS Generation by Nanoparticles of ZnO, J. Phys. Chem. C, **113**, 15997–16001(2009).
88. E. Alpaslan, B. M.Geilich, H.Yazici, T. J. Webster, pH-Controlled Cerium Oxide Nanoparticle Inhibition of Both Gram-Positive and Gram-Negative Bacteria Growth, Scientific Reports,**7**, 45859 (2017).
89. E. Alpaslan, H. Yazici, N. H. Golshan, K. S. Ziemer, T. J. Webster, pH-Dependent Activity of Dextran-Coated Cerium Oxide Nanoparticles on Prohibiting Osteosarcoma Cell Proliferation, ACS Biomater. Sci. Eng. **1**, 1096−1103 (2015).
90. A. Asati, S. Santra, C. Kaittanis, S. Nath, J. M. Perez, Oxidase like activity of polymer-coated cerium oxide nanoparticles. Angew. Chem., Int. Ed. **48**, 2308−12(2009)
91. J. M. Dowding, S. Das, A. Kumar, T. Dosani, R. McCormack, A. Gupta, Cellular interaction and toxicity depend on physicochemical properties and surface modification of redox-active nanomaterials. ACS Nano, **7**, 4855−68 (2013)

92. A. S. Karakoti, N. A. Monteiro-Riviere, R. Aggarwal, J. P. Davis, R. J. Narayan, Self, W. T.; et al. Nanoceria as antioxidant: Synthesis and biomedical applications. JOM 2008, 60, 33−7
93. D. Dutta, R. Mukherjee, S. Ghosh, M. Patra, M. Mukherjee, T. Basu, ACS Appl. Nano Mater., (2022) **https://doi.org/10.1021/acsanm.1c04518**.
94. T. M. Benn, P. Westerhoff, Nanoparticle Silver Released into Water from Commercially Available Sock Fabrics. Environ. Sci. Technol. **42**, 4133−4139 (2008).
95. Y. Zhao, Y. Tian, Y. Cui, W. Liu, W. Ma, X. Jiang, Small Molecule-Capped Gold Nanoparticles as Potent Antibacterial Agents That Target Gram-Negative Bacteria. J. Am. Chem. Soc. **132**, 12349−12356 (2010).
96. M. Ahamed, Toxic Response of Nickel Nanoparticles in Human Lung Epithelial A549 Cells. Toxicol. Vitro.**25**, 930−936 (2011).
97. R. Long, Y. Dai, G. Meng, B. Huang, Energetic and Electronic Properties of X- (Si, Ge, Sn, Pb) Doped TiO_2 from First-Principles. Phys. Chem. Chem. Phys. **11**, 8165−8172 (2009).
98. V. Etacheri, G. Michlits, M.K. Seery, S.J. Hinder, S.C. Pillai, A highly efficient $TiO_{2-x}C_x$ nano-heterojunction photocatalyst for visible light induced antibacterial applications. ACS Appl Mater Interfaces **5**, 1663–1672 (2013).
99. T. Gordon, M. Kopel, J. Grinblat, E. Banin, S. Margel, New synthesis, characterization and antibacterial properties of porous ZnO and C-ZnO micrometre-sized particles of narrow size distribution, J. Mater. Chem. **22**, 3614 (2012).
100. C. Hanley, J. Layne, Punnoose, A., Reddy, K. M., Coombs, I., Coombs, A.,Feris, K., Wingett, D. Preferential Killing of Cancer Cells and Activated Human T cells using ZnO. Nanotechnology.**19**, 295103 (2008).
101. P. Thevenot, J. Cho, D. Wavhal, R. B. Timmons, L.Tang, Surface Chemistry Influences Cancer Killing Effect of TiO_2 Nanoparticles. Nanomedicine **4**, 226–36 (2008).
102. J. J. Liu, X. L. Fu, S. F. Chen, Y. F. Zhu, Electronic structure and optical properties of Ag_3PO_4 photocatalyst calculated by hybrid density functional method, Appl. Phys. Lett. **99**, 191903 (2011).
103. M. Grätzel, Photoelectrochemical Cells. Nature **414**, 338–344 (2001).
104. C.D. Vecitis, K.R. Zodrow, S. Kang, M. Elimelech, Electronic Structure-Dependent Bacterial Cytotoxicity of Single-Walled Carbon Nanotubes. ACS Nano **4**, 5471–5479 (2010).
105. F. Dong, X. Xiao, G. Jiang, Z. Yuxin, W. Cui, J. Ma. Surface oxygen-vacancy induced photocatalytic activity of $La(OH)_3$ nanorods prepared by a fast and scalable method Phys. Chem Chem Phys **17**,16058 (2015).
106. M.A. Butler, D.S Ginley, Prediction of Flatband Potentials at Semiconductor-Electrolyte Interfaces from Atomic Electronegativities. J.Electrochem. Soc. **125**, 228–232 (1978).
107. V. A. Mëiìamlin, I. V. Pleskov, Electrochemistry of Semiconductors; Plenum Press: New York, USA, 1980.
108. Y. Xu, M.A.A. Schoonen, The Absolute Energy Positions of Conduction and Valence Bands of Selected Semiconducting Minerals. Am. Mineral. **85**, 543–556 (2000).
109. A. Fujishima, T. N. Rao, D. A. Tryk, Titanium dioxide Photocatalysis J. Photochem. Photobiol. C: Photochem. ReV. **1**, 1–21 (2000).
110. A. Lipovsky, Z. Tzitrinovich, H. Friedmann, G. Applerot, A. Gedanken, R. Lubart, EPR Study of Visible Light-Induced ROS Generation by Nanoparticles of ZnO. J. Phys. Chem. C **113**, 15997−16001 (2009)
111. G. Applerot, A. Lipovsky, R. Dror, N. Perkas, Y. Nitzan, R. Lubart, A. Gedanken, Enhanced antibacterial activity of nanocrystalline ZnO due to increased ROS-mediated cell injury. Adv. Funct. Mater. **19**, 842−852 (2009).

112. N. Jones, B. Ray, K. T. Ranjit, A. C. Manna, Antibacterial Activity of ZnO Nanoparticle Suspensions on a Broad Spectrum of Microorganisms. FEMS Microbiol. Lett. **279**, 71−76 (2008).
113. A. Sapkota, A. J. Anceno, S. Baruah, O. V. Shipin, J. Dutta, Zinc Oxide Nanorod Mediated Visible Light Photoinactivation of Model Microbes in Water. Nanotechnology **22**, 215703 (2011).
114. X. Xu, D. Chen, Z. Yi, M. Jiang, L. Wang, Z., Zhou, Fan., Y.Wang, D. Hui, Antibacterial Mechanism Based on H_2O_2 Generation at Oxygen Vacancies in ZnO Crystals. Langmuir **29**, 5573−5580 (2013).
115. T. O. Okyay, R. K. Bala, H. N. Nguyen, R. Atalay, Y. Bayam, F. D. Rodrigues, Antibacterial properties and mechanisms of toxicity of sonochemically grown ZnO nanorods, RSC Adv., **5**, 2568 (2015).
116. S. Ghosh, V.S. Goudar, K.G. Padmalekha, S.V. Bhat, S. S. Indi, H.N. Vasan, ZnO/Ag nanohybrid: synthesis, characterization, synergistic antibacterial activity and its mechanism. RSC Adv. **2**, 930–940 (2012)
117. A. Janotti, C. G. Van de Walle, Oxygen vacancies in ZnO, Appl. Phys. Lett. **87**, 122102 (2005).
118. P. Bhadra, M.K. Mitra, G.C. Das, R. Dey, S. Mukherjee, Interaction of chitosan capped ZnO nanorods with Escherichia coli, Materials Science and Engineering C **31**, 929–937 (2011).
119. T. Jansson, Z. J. Clare-Salzler, T. D. Zaveri, S. Mehta, N. V. Dolgova, B.-H. Chu, Ren, F.,Keselowsky, B. G. J..Nanosci. Nanotechnol., **12**, 7132–7138 (2012)
120. A. Azam, A. S. Ahmed, M. Oves, M. S. Khan, S. S. Habib, A. Memic, Antimicrobial Activity of Metal oxide Nanoparticles against Gram-positive and Gram-negative bacteria: a comparative study. Int. J. Nanomed.,**7**, 6003–6009 (2012)
121. G. Applerot, N. Perkas, G. Amirian, O. Girshevitz, A. Gedanken, Sonochemical co-deposition of antibacterial nanoparticles and dyes on textiles. Appl. Surf. Sci., **256**, S3 –S8 (2009).
122. S. H. Hwang, J. Song, Y. Jung, O. Y. Kweon, H. Song, J. Jang, Electrospun ZnO/TiO_2 composite nanofibers as a bactericidal agent, Chem. Commun. **47**, 9164–9166 (2011).
123. R. Brayner, R. Ferrari-Iliou, N. Brivois, S. Djediat, M. Benedetti, F. Fievet, Toxicological Impact Studies Based on Escherichia coli Bacteria in Ultrafine ZnO Nanoparticles Colloidal Medium. Nano Lett. **6**, 866−870 (2006).
124. M. Li, L. Zhu, D. Lin, Toxicity of ZnO Nanoparticles to Escherichia coli: Mechanism and the Influence of Medium Components. Environ. Sci. Technol. **45**, 1977−1983 (2011).
125. S. Singh, K.C. Barick, D. Bahadur, Shape-controlled hierarchical ZnO architectures: photocatalytic and antibacterial activities. CrystEng Comm **15**, 4631–4639 (2013).
126. M. Bus¸ila ˇ, V. Mus¸at, T. Textor, B. Mahltig, Synthesis and characterization of antimicrobial textile finishing based on Ag:ZnO nanoparticles/chitosan biocomposites. RSC Adv **5**, 21562–21571 (2015).
127. X. Liang, M. Sun, L. Li, R. Qiao, K. Chen, Q. Xio, F. Xu, Preparation and antibacterial activities of polyaniline/$Cu_{0.05}Zn_{0.95}O$ nanocomposites. Dalton Trans **41**, 2804–2811 (2012).
128. Y.W. Wang, A. Cao, Y. Jiang, X. Zhang, J. H. Liu, Y. Liu, H. Wang, Superior Antibacterial Activity of Zinc Oxide/Graphene Oxide Composites Originating from High Zinc Concentration Localized around Bacteria, ACS Appl. Mater. Interfaces **6**, 2791−2798 (2014).

129. N. C. Raut, T. Mathews, P. K. Ajikumar, R. P. George, S. Dash, A. K. Tyagia, Sunlight active antibacterial nanostructured N-doped TiO_2 thin films synthesized by an ultrasonic spray pyrolysis technique, RSC Advances, **2**, 10639–10647 (2012).
130. W. Xiao, J. Xu, X. Liu, Q. Hu, J. Huang, Antibacterial hybrid materials fabricated by nanocoating of microfibril bundles of cellulose substance with titania/chitosan/silver-nanoparticle composite films, J. Mater. Chem. B, **1**, 3477 (2013).
131. X. Liu, Y. Luo, T. Wu, J.Huang, Antibacterial activity of hierarchical nanofibrous titania–carbon composite material deposited with silver nanoparticles, New J. Chem. **36**, 2568–2573 (2012).
132. H. Kong, J. Song, J. Jang, One-step fabrication of magnetic c-Fe_2O_3/polyrhodanine nanoparticles using in situ chemical oxidation polymerization and their antibacterial properties, Chem. Commun., **46**, 6735–6737 (2010).
133. J. Liu, Z. Zhao, H. Feng, F. Cui, One-pot synthesis of Ag–Fe_3O_4 nanocomposites in the absence of additional reductant and its potent antibacterial properties, J. Mater. Chem., **22**, 13891 (2012).
134. I. Perelshtein, G. Applerot, N. Perkas, E. Wehrschuetz-Sigl, A. Hasmann, G. Guebitz, A. Gedanken, CuO –cotton Nanocomposite: Formation, Morphology and Antibacterial Activity. Surf. Coat. Technol., **204**, 54 (2009).
135. O. Akhavan, R. Azimirad, S. Safad, E. Hasanie, CuO/$Cu(OH)_2$ hierarchical nanostructures as bactericidal photocatalysts, J. Mater. Chem. **21**, 9634–9640 (2011).
136. S. Purwajanti, L. Zhou, Y. A. Nor, J. Zhang, H. Zhang, X. Huang, C.Yu, Synthesis of Magnesium Oxide Hierarchical Microspheres: A Dual-Functional Material for Water Remediation. ACS Appl. Mater. Interfaces **7**, 21278−21286 (2015).
137. M.R. Bindhu, M. Umadevi, M. K. Micheal, M. V. Arasu, N. A. Al-Dhabi, Structural, morphological and optical properties of MgO nanoparticles for antibacterial applications. Materials Letters. **166**, 19–22 (2016).
138. Y. Cai, C. Li, D. Wu, W. Wang, F. Tan, X.Wang, P. K. Wong, X. Qiao, Highly active MgO nanoparticles for simultaneous bacterial inactivation and heavy metal removal from aqueous solution. Chemical Engineering Journal. **312**, 158–166 (2017).
139. M. Azimzadehirani, M.R. Elahifard, S. Haghighic, M. R. Gholami, Highly efficient hydroxyapatite/TiO_2 composites covered by silver halides as E. coli disinfectant under visible light and dark media, Photochem. Photobiol. Sci., **12**, 1787 (2013).
140. M. Eshed, J. Lellouche, S. Matalon, A. Gedanken, E. Banin, Sonochemical Coatings of ZnO and CuO Nanoparticles Inhibit Streptococcus mutans Biofilm Formation on Teeth Model, Langmuir. **28**, 12288−12295 (2012).
141. W. He, H.-K. Kim, W. G. Wamer, D. Melka, J. H. Callahan, J. J. Yin, Photogenerated Charge Carriers and Reactive Oxygen Species in ZnO/Au Hybrid Nanostructures with Enhanced Photocatalytic and Antibacterial Activity. J Am Chem Soc. **136**,750–757 (2014).
142. N. Perkas, A. Lipovsky, G. Amirian, Y. Nitzan, A. Gedanken, Biocidal properties of TiO_2 powder modified with Ag nanoparticles, J. Mater. Chem. B **1**, 5309 (2013).
143. A. Ray Chowdhuri, S. Tripathy, S. Chandra, S. Roy, S. K. Sahu, A ZnO decorated chitosan–graphene oxide nanocomposite shows significantly enhanced antimicrobial activity with ROS generation, RSC Adv. **5**, 49420 (2015).
144. S. Podder, S. Paul, P. Basak, B. Xie, N. J. Fullwood, S. J. Baldock, Y.Yang, J.G. Hardy, C.K. Ghosh, Bioactive Silver Phosphate/Polyindole Nanocomposites, RSC Advances, **10**,11060-11073 (2020).
145. W. Zhang, S. Hu, J.J. Yin, W. He, W. Lu, M. Ma, N. Gu, Y. Zhang. Prussian Blue Nanoparticles as Multienzyme Mimetics and Reactive Oxygen Species Scavengers. J. Am. Chem. Soc. **138**, 5860−5865 (2016).

146. T. Hamasaki, T. Kashiwagi, T. Imada, N. Nakamichi, S. Aramaki, K. Toh, S. Morisawa, H. Shimakoshi, Y. Hisaeda, S. Shirahata, Kinetic Analysis of Superoxide Anion Radical Scavenging and Hydroxyl Radical-Scavenging Activities of Platinum Nanoparticles. Langmuir **24**, 7354-7364 (2008).
147. B. K. Pierscionek, Y. B. Li, A. A. Yasseen, L. M. Colhoun, R. A. Schachar, W. Chen, Nanoceria have No Genotoxic Effect on Human Lens Epithelial Cells. Nanotechnology **21**, 035102 (2010).
148. Q. An, C. Sun, D. Li, K. Xu, J. Guo, C. Wang, Peroxidase-Like Activity of Fe_3O_4@Carbon Nanoparticles Enhances Ascorbic Acid-Induced Oxidative Stress and Selective Damage to PC-3 Prostate Cancer Cells. ACS Appl. Mater. Interfaces.**5**, 13248−13257 (2013).
149. C. K. Kim, T. Kim, I. Y. Choi, M. Soh, D. Kim, Y. J. Kim, H. Jang, H. S. Yang, J. Y. Kim, H. K. Park, S. P. Park, S. Park, T. Yu, B. W. Yoon, S. H. Lee, T. Hyeon, Ceria Nanoparticles that can Protect against Ischemic Stroke. Angew. Chem., Int. Ed. **51**, 11039−11043 (2012).
150. S. S. Lee, W. S. Song, M. J. Cho, H. L. Puppala, P. Nguyen, H. G. Zhu, L. Segatori, V. L. Colvin, Antioxidant Properties of Cerium Oxide Nanocrystals as a Function of Nanocrystal Diameter and Surface Coating. ACS Nano **7**, 9693−9703 (2013).
151. F. Pagliari, C. Mandoli, G. Forte, E. Magnani, S. Pagliari, G. Nardone, S. Licoccia, M. Minieri, P. D. Nardo, E. Traversa, Cerium Oxide Nanoparticles Protect Cardiac Progenitor Cells from Oxidative Stress. ACS Nano **6**, 3767−3775 (2012).
152. P. T. Xu, B. W. Maidment, V. Antonic, I. L. Jackson, S. Das, A. Zodda, X. Zhang, S. Seal, Z. Vujaskovic, Cerium Oxide Nanoparticles: A Potential Medical Countermeasure to Mitigate Radiation-Induced Lung Injury in CBA/J Mice. Radiat. Res. **185**, 516−526 (2016).
153. H. Wei, E. Wang, Nanomaterials with Enzyme-Like Characteristics (nanozymes): Next-Generation Artificial Enzymes. Chem. Soc. Rev. **42**, 6060−6093 (2013).
154. E. G. Heckert, S. Seal, W. T. Self, Fenton-Like Reaction Catalyzed by the Rare Earth Inner Transition Metal Cerium. Environ. Sci. Technol., **42**, 5014–5019 (2008).
155. Z. Tian, X. Li, Y. Ma, T. Chen, D. Xu, B.Wang, Y. Qu, Y. Gao, Quantitatively Intrinsic Biomimetic Catalytic Activity of Nanocerias as Radical Scavengers and Their Ability against H_2O_2 and Doxorubicin-Induced Oxidative Stress. ACS Appl. Mater. Interfaces **9**, 23342−23352 (2017).
156. M. Das, S. Patil, N. Bhargava, J. F. Kang, L. M. Riedel, S. Seal, J. J. Hickman, Auto-catalytic ceria nanoparticles offer neuroprotection to adult rat spinal cord neurons Biomaterials, **28**, 1918–1925 (2007).
157. D. Schubert, R. Dargusch, J. Raitano, S. W. Chan, Cerium and yttrium oxide nanoparticles are neuroprotectiveBiochem. Biophys. Res. Commun. **342**, 86–91 (2006).
158. R. W. Tarnuzzer, J. Colon, S. Patil, S. Seal, Vacancy Engineered Ceria Nanostructures for Protection from Radiation-Induced Cellular Damage Nano Lett. **5**, 2573–2577 (2005).
159. J.Colon, L. Herrera, J. Smith, S. Patil, C. Komanski, P. Kupelian, S. Seal, D. W. Jenkins, C. H. Baker, Protection from Radiation-induced Pneumonitis using Cerium Oxide Nanoparticles. Nanomed.: Nanotechnol., Biol. Med., **5**, 225–231 (2009).
160. S.A. Hosseini, M. Saidijam, J. Karimi, *et al.* Cerium Oxide Nanoparticle Effects on Paraoxonase-1 Activity and Oxidative Toxic Stress Induced by Malathion: A Potential Antioxidant Compound, Yes or No?. Ind J Clin Biochem **34,** 336–341 (2019)
161. A. P. Nagvenkar, A. Gedanken, $Cu_{0.89}Zn_{0.11}O$, A New Peroxidase-Mimicking Nanozyme with High Sensitivity for Glucose and Antioxidant Detection,ACS Appl. Mater. Interfaces **8**, 22301−22308 (2016).

162. K.T. Kitchin, S. Stirdivant, B.L. Robinette, *et al.* Metabolomic effects of CeO_2, SiO_2 and CuO metal oxide nanomaterials on HepG2 cells. Part Fibre Toxicol **14,** 50 (2017)
163. B.A. Rzigalinski, K. Meehan, R.M. Davis, Y. Xu, W.C. Miles, C.A. Cohen, Radical nanomedicine, Future Medicine. **1** (4) 399–412 (2006).
164. C. Korsvik, S. Patil, S. Seal, W.T. Self, Superoxide dismutase mimetic properties exhibited by vacancy engineered ceria nanoparticles, Chem. Commun. 10, 1056–1058 (2007)
165. A. Asati, S. Santra, C. Kaittanis, S. Nath, J.M. Perez, Oxidase-like activity of polymer-coated cerium oxide nanoparticles, Angew. Chem. Int. Ed. **48**, 2308–2312 (2009)
166. Z. Li, X. Yang, Y. Yang, Y. Tan, Y. He, M. Liu, et al., Peroxidase-mimicking nanozyme with enhanced activity and high stability based on metal–support interactions, Chem. Eur. J. **24** 409–415 (2018).
167. M. Shokrzadeh, H. Abdi, A. Asadollah-Pour, F. Shaki, Nanoceria attenuated high glucose-induced oxidative damage in HepG2 cells, Cell J. **18** 97 (2016).
168. A. Hosseini, M. Baeeri, M. Rahimifard, M. Navaei-Nigjeh, A. Mohammadirad, N. Pourkhalili, et al., Antiapoptotic effects of cerium oxide and yttrium oxide nanoparticles in isolated rat pancreatic islets, Hum. Exp. Toxicol. **32** 544–553 (2013)
169. R.W. Tarnuzzer, J. Colon, S. Patil, S. Seal, Vacancy engineered ceria nanostructures for protection from radiation-induced cellular damage, Nano Lett. **5** 2573–2577 (2005).
170. D. Oro, ´ T. Yudina, G. Fern´ andez-Varo, E. Casals, V. Reichenbach, G. Casals, et al., Cerium oxide nanoparticles reduce steatosis, portal hypertension and display antiinflammatory properties in rats with liver fibrosis, J. Hepatol. **64**, 691–698 (2016).
171. F. Caputo, M. De Nicola, A. Sienkiewicz, A. Giovanetti, I. Bejarano, S. Licoccia, et al., Cerium oxide nanoparticles, combining antioxidant and UV shielding properties, prevent UV-induced cell damage and mutagenesis, Nanoscale. **R 7** 15643–15656 (2015).
172. M. A. Saifi, S. Seal, C. Godugu, Nanoceria, the versatile nanoparticles: Promising biomedical applications, Journal of Controlled Release **338** 164–189 (2021)
173. M. J. Akhtar, M. Ahamed, H. A. Alhadlaq, M.A. Majeed Khan, S. A. Alrokayan, Glutathione replenishing potential of CeO_2 nanoparticles in human breast and fibrosarcoma cells, Journal of Colloid and Interface Science, **453**, 21-27 (2015)
174. L. Rubio, B. Annangi, L. Vila, A. Hernández, R. Marcos, Antioxidant and anti-genotoxic properties of cerium oxide nanoparticles in a pulmonary-like cell system, Arch Toxicol, **90**, 269–278 (2016)
175. Y. Yamakoshi, N. Umezawa, A. Ryu, K. Arakane, N. Miyata, Y. Goda, T. Masumizu, T. Nagano, Active Oxygen Species Generated from Photoexcited Fullerene (C_{60}) as Potential Medicines: $O_2^{\cdot -}$ versus $^1O_2$. J. Am. Chem. Soc. **125**, 12803-12809 (2003)
176. L. L. Dugan, D. M. Turetsky, C. Du, D. Lobner, M. Wheeler, C. R. Almli, C. K. F. Shen, T. Y. Luh, D. W. Choi, T. S. Lin, Carboxyfullerenes as neuroprotective agents, Proc. Natl. Acad. Sci. U. S. A., **94**, 9434–9439 (1997).
177. I. C. Wang, L. A. Tai, D. D. Lee, P. P. Kanakamma, C. K. F. Shen, T.-Y. Luh, C. H. Cheng, K. C. Hwang, C_{60} and Water-Soluble Fullerene Derivatives as Antioxidants Against Radical-Initiated Lipid Peroxidation J. Med. Chem. **42**, 4614–4620 (1999).
178. Y. L. Lai, P. Murugan, K. C. Hwang, Fullerene derivative attenuates ischemia-reperfusion-induced lung injury. Life Sci. **72**, 1271–1278 (2003).
179. N. Gharbi, M. Pressac, M. Hadchouel, H. Szwarc, S. R. Wilson, F. Moussa, Fullerene is a Powerful Antioxidant in Vivo with No Acute or Subacute ToxicityNano Lett. **5**, 2578–2585 (2005).
180. K. L. Quick, S. S. Ali, R. Arch, C. Xiong, D. Wozniak, L.L.A. Dugan, Carboxyfullerene SOD mimetic improves cognition and extends the lifespan of miceNeurobiol. Aging, **29**, 117–128 (2008).

181. R. B. Rainer, M. Vallant, M. Najam-ul-Haq, M. Rainer, Z. Szabo, W G. HuckChristian, K. Bonn, Medicinal applications of fullerenes, Int. J. Nanomedicine. **2**, 639–649 (2007).
182. G. Buettner, B. A. Jurkiewicz, Chemistry and Biochemistry of Ascorbic Acid. In Handbook of Antioxidants; Marcel Dekker: New York, 91-115 (1996).
183. J.J. Yin, P. P. Fu, H. Lutterodt, Y.T. Zhou, W. E. Antholine, W. Wamer, Dual Role of Selected Antioxidants Found in Dietary Supplements: Crossover between Anti- and Pro-Oxidant Activities in the Presence of Copper,J. Agric. Food Chem. **60**, 2554−2561 (2012).
184. M. Lu, Y. Zhang, Y. Wang, M. Jiang, X.Yao, Insight into Several Factors that Affect the Conversion between Antioxidant and Oxidant Activities of Nanoceria. ACS Appl. Mater. Interfaces **8**, 23580−23590 (2016).
185. Y. Chong, C. Ge, G. Fang, X. Tian, X. Ma, T. Wen, W. G. Wamer, C. Chen, Z. Chai, J. J.Yin, Crossover between Anti and Pro-oxidant Activities of Graphene Quantum Dots in the Absence or Presence of Light. ACS Nano **10**, 8690−8699 (2016).
186. J. Gupta, P. Bhargava, D. Bahadur, Fluorescent ZnO for imaging and induction of DNA fragmentation and ROS-mediated apoptosis in cancer cells, J. Mater. Chem. B, **3**, 1968 (2015).
187. Q. Zhao, J. Li, X. Zhang, Z. Li, Y.Tang, Cationic Oligo (thiophene ethynylene) with Broad-Spectrum and High Antibacterial Efficiency under White Light and Specific Biocidal Activity against S. aureus in Dark, ACS Appl. Mater. Interfaces **8**, 1019−1024 (2016).
188. Z.Han, X. Wang, C. Heng, Q. Han, S. Cai, J. Li, C. Qi, W.Liang, R.Yang, C. Wang, Synergistically enhanced photocatalytic and chemotherapeutic effects of aptamer-functionalized ZnO nanoparticles towards cancer cells, Phys. Chem. Chem. Phys. **17**, 21576-21582 (2015).
189. L. Chen, M. Liu, Q. Zhou, Recent developments of mesoporous silica nanoparticles in biomedicine. emergent mater. **3,** 381–405 (2020)
190. J.-h. Li, X.-r. Liu, Y. Zhang, F.-f. Tian, G.-y. Zhao, Q.-l.-y. Yu, F.-l. Jiang, Y. Liu. Toxicity of nano zinc oxide to mitochondria. Toxicol. Res., **1**, 137–144 (2012).
191. M. Premanathan, K. Karthikeyan, K. Jeyasubramanian, G. Manivannan, Selective toxicity of ZnO nanoparticles toward Gram-positive bacteria and cancer cells by apoptosis through lipid peroxidation , Nanomedicine, **7**, 184–192 (2011).
192. S. Ostrovsky, G. Kazimirsky, A. Gedanken, C. Brodie, Selective cytotoxic effect of ZnO nanoparticles on glioma cells Nano Res. **2**, 882–890 (2009).
193. B. D. Berardis, G. Civitelli, M. Condello, P. Lista, R. Pozzi, G. Arancia, S. Meschini, Exposure to ZnO nanoparticles induces oxidative stress and cytotoxicity in human colon carcinoma cells,Toxicology and Applied Pharmacology. **246**,116–127 (2010).
194. H. Yin, P. S. Casey, M. J. McCall, M. Fenech. Effects of Surface Chemistry on Cytotoxicity, Genotoxicity, and the Generation of Reactive Oxygen Species Induced by ZnO Nanoparticles,Langmuir **26**, 15399–15408 (2010).
195. T.K. Hong, N. Tripathy, H. J. Son, K.T. Ha, H.S. Jeong, Y.B.A Hahn, comprehensive in vitro and in vivo study of ZnO nanoparticles toxicity, J. Mater. Chem. B, **1**, 2985 (2013).
196. K. Krishnamoorthy, J. Yong Moon, H. Hyun, S. K. Cho, S. J. Kim, Mechanistic investigation on the toxicity of MgO nanoparticles toward cancer cells. J. Mater. Chem. **22**, 24610 (2012).
197. M. J. Akhtar, H.A. Alhadlaq, A. Alshamsan, M.A. Majeed Khan, M. Ahamed Aluminum doping tunes band gap energy level as well as oxidative stress-mediated cytotoxicity of ZnO nanoparticles in MCF-7 cells. Sci Rep. 5, 13876 (2015)
198. Y. Yang, Z. Song, W. Wu, A. Xu, S. Lv, S. Ji, Front Pharmacol. (2020) https://doi.org/10.3389/fphar.2020.00131

199. M. Ahamed, M. J. Akhtar, M.M. Khan, H. A Alhadlaq, SnO_2-Doped ZnO/Reduced Graphene Oxide Nanocomposites: Synthesis, Characterization, and Improved Anticancer Activity via Oxidative Stress Pathway, International Journal of Nanomedicine **16**, 89–104 (2021)
200. Y. Hou, A. Mushtaq, Z. Tang, E. Dempsey, Y. Wu, Y. Lu, C. Tian, J. Farheen, X. Kong, M. Z. Iqbal, Journal of Science: Advanced Materials and Devices. (2021) https://doi.org/ 10.1016/j.jsamd.2022.100417
201. P.C. Nagajyothi, P. Muthuraman, C.O. Tettey, K. Yoo , J. Shim, In vitro anticancer activity of eco-friendly synthesized ZnO/Ag nanocomposites, Ceramic International, **47**(15), 34940-34948 (2021)